10-1-1995

Spectroscopic and sensitometric studies of chemically produced silver clusters

Shilin Guo

Spectroscopic and Sensitometric Studies of Chemically Produced Silver Clusters

Shilin Guo

B.S. Canisius College, Buffalo, New York
(1993)

A thesis submitted in partial fulfillment of the requirements for the degree of Master of Science in the Center for Imaging Science, Rochester Institute of Technology

October 1995

Signature of the Author Shilin Guo

Accepted by Dana G. Marsh Oct. 27, 1995
Coordinator, M. S. Degree Program Date

Center for Imaging Science
Rochester Institute of Technology
Rochester, New York

Certificate of Approval
M. S. Degree Thesis

The M. S. degree thesis of Shilin Guo
has been examined and approved by the thesis committee as satisfactory for the thesis requirement for the Master of Science degree.

Prof. Richard K. Hailstone, Thesis Advisor

Dr. Cesare Verdi

Mr. Gary DiFrancesco

10/26/95
Date

Thesis Release Permission Form

Center for Imaging Science
Rochester Institute of Technology
Rochester, New York

Title of Thesis:

Spectroscopic and Sensitometric Studies of Chemically Produced Silver Clusters

I, Shilin Guo, hereby grant permission to the Wallace Memorial Library of R.I.T. to reproduce this thesis in whole or in part. Any reproduction will not be for commercial use or profit.

Signature: Shilin Guo

Date: 10/26/95

Spectroscopic and Sensitometric Studies of Chemically Produced Silver Clusters

Shilin Guo

Submitted in partial fulfillment of the requirements for the degree of Master of Science in the Center for Imaging Science, Rochester Institute of Technology

Abstract:

This thesis research uses 0.45 μm octahedral AgBr emulsion to study chemically produced silver clusters. Reduction sensitization has been carried out with DMAB, $SnCl_2$, and NaOH. The progress of the reaction has been monitored both with sensitometry and diffuse reflectance spectra of the chemically produced silver clusters. The reflection minimum occurs at about 476 nm, independent of reagent. The absorbency by these clusters, derived from the Kubelka-Munk transform, is related to the concentration of the sensitizing agent. Exposure to light causes a decrease in the absorbency by these silver clusters, indicating that some of the silver clusters are hole traps. However, these silver clusters cannot be completely photobleached -- indicating some of them may be electron traps.

Acknowledgments

The author would like to extend her appreciation and thanks to Professor Richard K. Hailstone, her thesis advisor. This study would not have been possible without his patience, knowledge, and guidance.

The author would like to extend her appreciation to Dr. Cesare Verdi of the 3M Technical Center. His guidance and encouragement have been a great asset and the author is very grateful for his time and patience.

The author would like to extend her appreciation to Mr. Gary DiFrancesco for his help and guidance, for precipitating the emulsions used in this thesis, and for ensuring that there was always an ample supply of chemistry and other consumables.

Table of Contents

List of Tables

List of Figures

Chapter 1

Introduction

Chemical sensitization is the treatment of the silver halide grain surface with a low level of sensitizing agents to increase the efficiency of latent image formation and/or to modify the photographic performance, such as D-logE curve shape, reciprocity failure, response to development time, etc. Such chemicals can react with the grain surface to form small silver clusters or ionic clusters. These clusters are called sensitizer centers. Evidence [Tani,1994] [Spencer, 1967] [Palm, 1977] [Spencer, 1968] [Spencer, 1983] [Collier, 1979] has shown that these sensitizer centers could either trap photoelectrons or photoholes, and thereby prevent recombination and greatly increase the quantum sensitivity of silver halide emulsions. Keen attention is being paid to the characterization of non-developable silver clusters acting as a positive hole trap or as an electron trap, which are referred to as R-center and P-center, respectively [Hamilton, 1981].

Traditionally, chemical sensitization has been divided into three categories: sulfur, sulfur + gold, and reduction sensitization. Previous investigators have suggested that sulfur sensitizer centers are silver sulfide aggregates $(Ag_2S)_n$ [Hamilton, 1984], and sulfur + gold sensitizer centers are a mixed complex of Ag^+, Au^+, and S^{2-} ions [Hirsch, 1972]. Both of them act as electron traps during exposure [Hamilton, 1984], but sulfur + gold

sensitization gives higher sensitivity than sulfur sensitization alone [Cash, 1983] and gold can also lead to an antifogging effect [Hirsch, 1972].

Reduction sensitizer centers are of great theoretical interest because they are silver centers, yet their properties have not been studied as thoroughly as sulfur sensitizer centers. Reduction sensitizers are reducing agents. They can donate electrons to silver ions, Ag^+, to form silver clusters:

$$Ag^+ + e^- = Ag^0 \qquad (1.1)$$

$$Ag^0 + Ag^+ + e^- = Ag_2^0 \ldots \qquad (1.2)$$

Since these silver clusters are stable but not developable, it is reasonable to say reduction sensitization centers are Ag_2, Ag_3, or Ag_4. Evidence indicates that reduction sensitization leads to the formation of sensitizer centers which can be either hole traps or electron traps [Tani, 1994] [Spencer, 1967] [Palm, 1977], depending on sensitizer concentration, reaction time, and temperature. P centers act as electron traps at positively charged sites and R centers act as positive hole traps at neutral sites [Tani, 1971].

Theoretically, sulfur + gold + reduction sensitization would greatly increase the quantum sensitivity of silver halide emulsions (see Table 1.1) [Hailstone, 1988], since sulfur + gold provides electron traps and R centers provide hole traps. However, S + Au + R sensitization has so far proven impractical. Over time the fog may increase due to coalescence of centers. In addition, the speed may decrease because there are fewer R centers. Also, large grains may suffer internal recombination, which surface R centers may not completely inhibit. These problems can not be solved unless a controlled way to produce R centers is known.

Table 1.1 Effect of S+Au and hydrogen hypersensitization * on quantum sensitivity.

Sensitization	Quantum Sensitivity (photons/grain)
Unsensitized	75-100 or more
S + Au	8-9
S + Au in vacuum + H_2	2-3

The purpose of this study was to characterize chemically produced silver centers, Ag_n. This thesis research puts emphasis on those produced by reducing agents. The reduction sensitizers used were borane-dimethylamine complex (DMAB), stannous chloride ($SnCl_2$), and high pH (NaOH). Theoretically, both DMAB and $SnCl_2$ are two electron donors upon heating. Reduction by high pH uses OH^- as an electron donor or pH-activated reducing impurities in the gelatin.

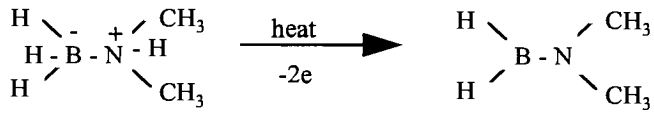

DMAB

(1.3)

* Hydrogen hypersensitization is generally considered to be an efficient form of reduction sensitization [Babcock, 1975]. It produces silver clusters, as detected by gold latensification [Hailstone, 1988]. Like reduction sensitization, hydrogen hypersensitization is expected to destroy photoholes [Spencer, 1983].

$$Sn^{2+} \xrightarrow[-2e^-]{\text{heat}} Sn^{4+} \qquad (1.4)$$

The properties of these silver clusters to be characterized are size n, reflectance or absorption spectra, and classification as R centers or P centers. Sensitometric properties of reduction-sensitized emulsions were also studied and correlated with their physical properties.

A summary of several previous investigations concerning reduction sensitization is presented in the next section. Then, the experimental section will outline the methodology. Results and discussion will then be presented. Finally, the main conclusions of this work will be summarized.

Chapter 2

Previous Investigations

Reduction sensitization of microcrystals or grains of an emulsion of a silver halide in an aqueous gelatin solution was first operationally defined by Lowe, Jones, and Roberts [Lowe, 1951]. Since that time there have been a number of studies of reduction sensitization, and a number of mechanisms have been proposed to explain the increase of grain sensitivity.

Spencer concluded that the important sensitizing product of reduction sensitization is silver [Spencer, 1967]. He found that when the reduction-sensitized emulsion is given the treatments used for gold latensification [♣] and then developed, either normally or with arrested development,[♦] a fraction of the grains is found to have been made developable, even without exposure. No development occurs if sulfur-sensitized or primitive grains are treated in the same way. The latent fog centers revealed by the gold treatment of the sensitized emulsion presumably mark points where discrete silver aggregates formed during the sensitization process.

♣ Gold latensification: treatment of a coating with gold solution ($KAuCl_4$ + KSCN) after exposure but before development to intensify latent image and increase speed. It was found by Hamilton that, in evaporated layers, smaller gold clusters than silver clusters can be physically developed [Hamilton, 1974]. Therefore, if latent image is partially gold, it would be expected to decrease n – the minimum developable size of silver cluster.

♦ Arresting developer: weak developer which can develop a grain partially at the site where the latent image formed.

The evidence for the production of silver during reduction sensitization is most convincing. In contrast, in the scientific literature, little attention has been paid to the processes which may precede silver cluster formation: adsorption of sensitizer, reduction of silver halide to silver, and rearrangement of atoms to form sensitizer centers. Even the stoichiometry and kinetics of the sensitizing reactions have not been discussed thoroughly. In addition, whether the inability of these sensitization specks to initiate development is a result merely of their small size, or whether other factors, such as structure, location, charge, etc., are involved is not well known, and the role of the silver clusters is not clear, although there is a general agreement that the silver clusters are either functioning as electron traps or as hole traps. Essentially, the purpose of the present work is to investigate the electronic properties of these chemically produced silver clusters. The following paragraphs outline several selected investigations relevant to this thesis.

Spencer found that at optimum sensitization many silver clusters per grain are produced [Spencer, 1981]. Fig. 2.1 is a plot of a representative distribution of centers determined for an octahedral AgBr emulsion with grains having an edge length of 0.9 μm. The centers were detected by the gold latensification and arrested-development technique [Spencer, 1967]. The number of development specks* found, however, increased with increasing time of gold bathing; thus, the specks portrayed in Fig. 2.1 represent only a fraction of the sensitizer centers. The Poisson values were determined from experimental values of mean number of

* Specks: gold latensification and arrested development make a silver halide grain partially developed at sites where latent subimage centers or chemically produced silver clusters form. Each of these centers forms a development speck which can be observed under an electron microscope.

specks per grain. He concluded that the reduction sensitization centers are distributed randomly among the grains.

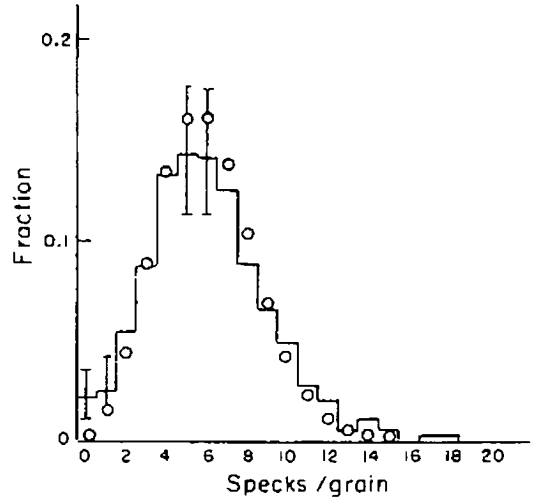

Fig. 2.1 Distribution of reduction sensitization specks among grains of an emulsion composed of octahedral grains of mean edge length of 0.9 μm. The sensitization conditions were: 0.1 mg DMAB per Ag mole, 30 min at 60 ℃. Development conditions: 5 min gold bathing, 5 min wash in KBr solution (1 g/l), 7 min EAA-6. Solid lines: experimental results; circles: Poisson values; line and bars: 95% confidence limits. (from [Spencer, 1981])

Spencer et. al. conducted a series of experiments in 1967 on reduction sensitization to prove that chemically produced Ag_n are hole traps [Spencer, 1967]. In their experiment, grains of reduction sensitized emulsion are exposed for four sec to low-intensity light, bathed in the latensifying solution for 20 min, and given the standard arrested development. The reduction sensitization specks and latent image specks -- or at least a fraction of them -- become visible in the electron microscope. The developed silver particles fall into two distinct size classes, one with a mean diameter about 0.1 of the grain diameter, and the other with a mean diameter about 0.4 of the grain diameter. The distribution of the large specks corresponds to that of the image centers, and the distribution of small specks to that of the fog.

Fig. 2.2 shows the effect of increasing exposure on the number of small and large specks in this emulsion. In this case, the average number of development centers/grain in the unexposed emulsion, when bathed for 20 min in the gold latensifying solution and developed, was 0.99. After an exposure of 4 sec to light of moderate intensity, an average of 1.31 small specks and 1.16 large specks per grain were observed. After an exposure of 8 sec to light of the same intensity, most of the small centers have disappeared, leaving essentially only large specks exhibiting a strong preference for an one-per-grain distribution.

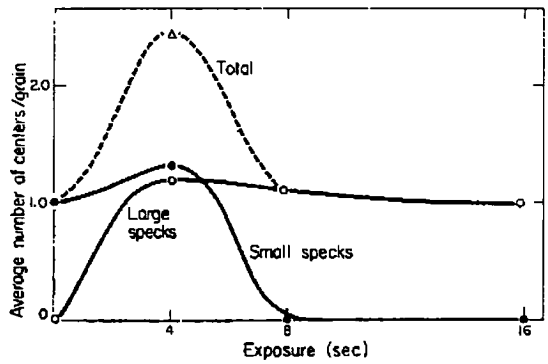

Fig. 2.2 Variation with time of exposure of the average number of specks per grain of a reduction-sensitized emulsion bathed in gold before development. ° Large specks. • Small specks. Δ Total specks. (from [Spencer, 1967])

These data show clearly the very important fact that the sensitizer products, which are capable of being made into developable centers by gold latensification, are progressively destroyed by exposure to light. This demonstrates conclusively that at least one function of the products of reduction sensitization is to combine with either photoholes or free halogen, thus protecting the growing latent image centers from regression. In this set of data, a latent image center has formed in most grains before the sensitizer products have been noticeably

diminished. It appears that latent image silver has formed at sites distinctly apart from those at which the fogging sensitizer specks are located. This indicates that the products of normal reduction sensitization are relatively unimportant as electron traps, but provide efficient hole traps.

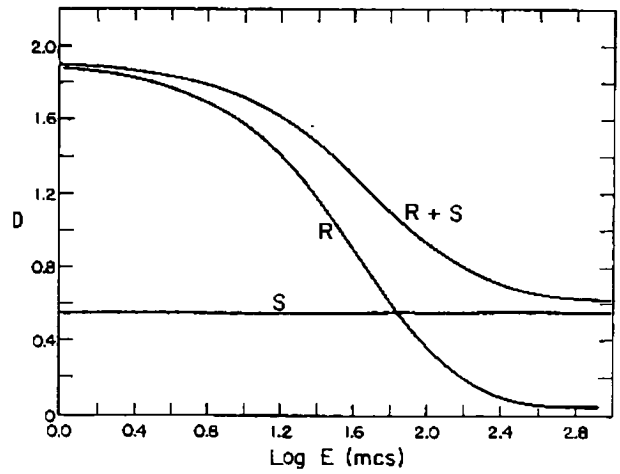

Fig. 2.3 D-logE curves for reduction- (R), sulfur- (S), and reduction-plus-sulfur- (R+S) sensitized grains, desensitized and bathed in gold. 2 mg of $SnCl_2$/Ag mole, 80 mg of $Na_2S_2O_3$/Ag mole, and 600 mg of phenosafranine/Ag mole were used for reduction sensitization, sulfur sensitization, and desensitization, respectively. Development in Kodak Developer DK-50 for 5 min at 20℃. (from [Spencer, 1968])

Later, Spencer also conducted a reduction-plus-sulfur sensitization experiment [Spencer, 1968]. The sensitization was accomplished by first reduction sensitizing, followed by sulfur sensitizing the liquid emulsion. A desensitizing dye, phenosafranine, was added to the emulsion to prevent latent image formation. Fig. 2.3 shows the D-logE curves for reduction-sensitized (R), sulfur-sensitized (S), and reduction-plus-sulfur-sensitized (R+S) grains. Because of the large amount of sulfur and reduction sensitizer, appreciable fog is exhibited for sulfur-, reduction-, and reduction-plus-sulfur sensitized grains. In the sulfur-sensitized grains, no effect of exposure is indicated. No latent image centers are formed, because of the

overriding effect of the large amount of phenosafranine. Also, the silver sulfide fog centers are not affected by the light exposure. Fog due to reduction sensitization can be completely photo-bleached, but fog caused by reduction-plus-sulfur sensitization only can be bleached to the density of the sulfur-sensitized grain. This experiment again shows that reduction sensitization center behavior is consistent with hole traps and that sulfur sensitizer centers are not oxidized by holes.

Tani in 1971 suggested that reduction sensitization ($SnCl_2$ and Ag^+ treatment of a 0.65 μm octahedral AgBr emulsion) forms both electron traps and hole traps [Tani, 1971]. He proposed to explain the difference between the hole trapping and electron trapping centers in terms of the sites at which they formed. He suggested that silver centers which formed at surface defect sites such as positive kinks would be charged and trap electrons, whereas those at defect-free sites would be electrostatically neutral and trap holes. According to this hypothesis, the distinction depends only upon the residence site and is independent of the number of silver atoms in the center. In 1972, Tani also found that on very small silver halide grains or on somewhat larger cubic ones, normal levels of reduction sensitization with $SnCl_2$ produced almost exclusively hole-trapping centers, but that prolonged reaction time, higher $SnCl_2$ concentrations, or reaction at low pAg also formed electron-trapping centers [Tani, 1972].

In 1977, Moisar and his coworkers confirmed Tani's hypothesis [Palm, 1977]. In their experiments, monodispersed cubic and octahedral AgBr emulsions were prepared by pAg-controlled double-jet method. Reduction sensitization was performed by reaction in the presence of hydrazine or at low pAg. After sensitization, the original emulsion conditions were

restored by pH and pAg readjustment. The emulsions were coated and the strips were exposed behind a step-wedge for 0.4 sec to white light. The exposed strips were developed either in a surface developer to obtain surface sensitivity or, after bleaching, in an internal developer containing thiosulphate as solvent to obtain intrinsic internal sensitivity.

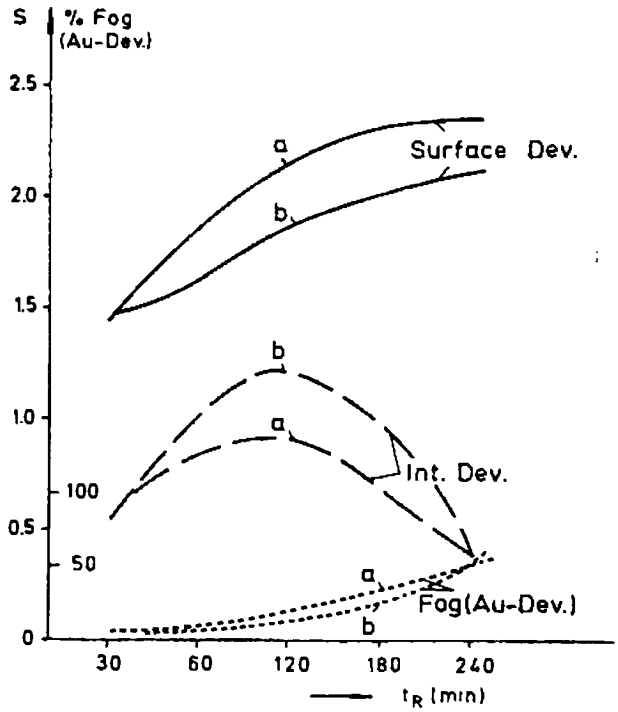

Fig. 2.4 Sensitivity for surface and internal development and fog after Au-development [4] vs time of reduction sensitization of a cubic AgBr emulsion. (a) Silver digestion at pAg 5.4 and 50 °C. (b) Digestion with 0.23 g hydrazine/mole AgBr at 50 °C. (from [Palm, 1977])

Their experiments, as shown in Fig. 2.4, indicate two very different regions appear in the course of reduction sensitization: there is one region which is observed in earlier stages of sensitization and/or under somewhat milder reaction conditions (high pAg, low temperature, smaller amount of reducing agent) and where both the surface and internal speeds increase

compared to those of the primitive emulsion. The other region appears after longer sensitization time and/or at more extreme sensitization conditions (low pAg, etc.). In this region, surface speed still remains high whereas the internal speed decreases.

In the early stage of reduction sensitization silver specks are formed which upon exposure cause a general increase of speed -- both surface and internal. Such specks obviously render the photographic process more efficient, but they do not act as sites where latent image deposits. Although, as a result of reduction, they are subdevelopable specks consisting of silver, they do not grow to developable size upon exposure. They therefore are not electron traps. However, since they increase speed they appear to be hole traps. By trapping and eliminating holes they decrease the chance of recombination, and thereby increase the lifetime and/or the number of electrons.* These electrons consequently lead to the formation of an increased amount of latent image silver. With increasing time of the sensitization reaction the sensitometric behavior changes: surface sensitivity increases, whereas the internal sensitivity drops sharply. This can only be explained by electron capture at the chemically produced clusters on the surface of the grain.

Reduction sensitization appears to lead to both types of traps. It is a matter of the reaction conditions determining if sensitization yields predominantly hole traps or if electron traps (perhaps in addition to many hole traps) are formed. Even if a great number of hole traps

---

♠ Au-Development: there is only a very slow increase of fog with sensitization time upon surface development. If, however, surface development is combined with a treatment in a gold decoration bath the fog is greatly increased and, at longer sensitization times, approaches nearly a value of 100%.

* An intriguing feature of reduction sensitization has been pointed out by Lowe [Lowe, 1963]. For silver centers of 2-atom size, either initially or bleached to that size by photooxidation, the following reaction may occur:

$$Ag_2 + h^+ \rightarrow Ag_2^+$$
$$Ag_2^+ \rightarrow Ag + Ag^+$$
$$Ag \rightarrow Ag^+ + e^-$$

By this mechanism, a single absorbed photon produces two conduction-band electrons.

exist in a grain, just one additional electron trap would decisively influence latent image topography. The hole traps in this case would indeed enhance the photographic yield by reducing recombination between holes and electrons, but the position of the latent image is determined by the electron trap, if such is present.

In 1979, Collier extended the work of Tani and Moisar et. al. using a 1.08 μm octahedral AgBr emulsion and included DMAB, $SnCl_2 \bullet 2H_2O$, hydrazine, high pH, and low pAg as reduction sensitizers [Collier, 1979]. Variations were made in the sensitizer concentration and temperature of reaction. She found that all sensitizations could produce a surface speed gain that was accompanied by increased electron trapping as monitored by microwave photoconductivity. Significant surface speed changes due to hole trapping were detected only with DMAB and $SnCl_2 \bullet 2H_2O$. These sensitizations produced hole traps at low sensitizer concentrations, and both hole and electron traps at higher concentration levels. With the increase in electron trapping, the evidence for hole trapping disappears.

In 1981, Hamilton and Baetzold studied the growth kinetics of development centers formed at gold-treated reduction sensitization centers and at small photolytic centers [Hamilton, 1981]. The result indicated that these two types of centers differ in some property other than size. Molecular orbital calculations support Tani's hypothesis that reduction sensitization centers usually form at uncharged sites, whereas photolytic silver centers are formed at partially charged kinks and jogs.

In 1994, Sydow et. al. studied the effect of exposure on the UV-visible spectra of ultra-fine-grained, chemically unsensitized emulsions, which were precipitated with various gelatin concentrations and which have different silver halide/gelatin proportions [Sydow, 1994]. The dried layers of these emulsions were made 0.5 mm thick, and were exposed to flash light (flash energy 960 J, color temperature 5500 K, flash time 0.001 s, distance 50 cm). Reflectance spectra were recorded for all specimens both before exposure and after exposure. By subtracting the reflectance spectra recorded after exposure from the reflectance spectra of the unexposed specimens, difference spectra were calculated, in which the changes of optical density due to photolysis of the silver halide becomes visible. Fig. 2.5 shows an example of such difference spectrum. The density difference δD between the exposed and unexposed layer is plotted against wave-number.

$$\delta D = D_{(exposed)} - D_{(unexposed)}$$

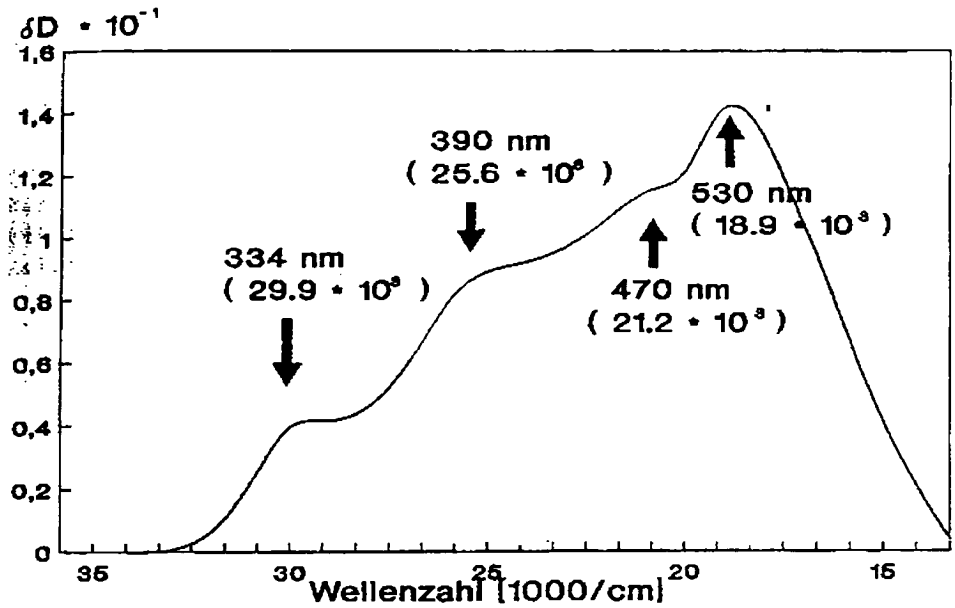

Fig. 2.5 Difference spectrum of an exposed AgBr emulsion layer. (from [Sydow, 1994])

Four photolysis bands can be seen in Fig. 2.5, situated at 334 ± 2 nm, 390 ± 6 nm, 470 ± 8 nm, and 530 ± 9 nm. Only the 530 nm band appeared in all the cases. By contrast, the 334 nm, the 390 nm, and the 470 nm photolysis bands frequently scarcely stood out from the noise. The difference spectrum in Fig. 2.5 was chosen as an example of one of the few cases in which all four photolysis bands could be seen.

Tani, also in 1994, used adsorbed Ag_n spectroscopy, accompanied by photoconductivity and sensitometry of the emulsion, to study reduction-sensitization-produced silver clusters [Tani, 1994]. Photographic emulsions used were composed of octahedral and cubic AgBr grains (diameter 0.2 μm) suspended in aqueous gelatin solution, and prepared by pAg controlled double jet method. Reduction sensitization was accomplished by reacting the emulsion with DMAB for 60 min at 60°C. These emulsions were coated, dried, and subjected to various measurement. Each film strip was exposed to a tungsten lamp (color temperature: 2854 K) through a continuous wedge for 10 sec and subjected to surface development at 20°C for 10 min by surface developer EAA-1 [James, 1953]. The photoconductivity of AgBr grains with photoelectrons as electronic carriers was given by the peak height of their microwave photoconductivity signal at -100°C. Absorption spectra of reduction sensitization centers, fog centers, and latent image centers on emulsion grains were obtained by measuring the reflectance of thick layers of reduction-sensitized emulsion in liquid state with reference to unexposed and unsensitized emulsion by means of a spectrophotometer with an integrating sphere.

Fig. 2.6 shows photographic sensitivity, fog density, and photoconductivity of reduction-sensitized an octahedral AgBr emulsion as a function of the amount of the DMAB

used. With increasing amount of sensitizer, the increase in sensitivity caused by reduction sensitization centers proceeded through two steps, and eventual formation of fog centers. The first step was not associated with change in photoconductivity, and was ascribed to the sensitization caused by R-centers (hole traps). The second step was associated with decrease in photoconductivity, and was ascribed to the sensitization caused by P-centers (electron traps).

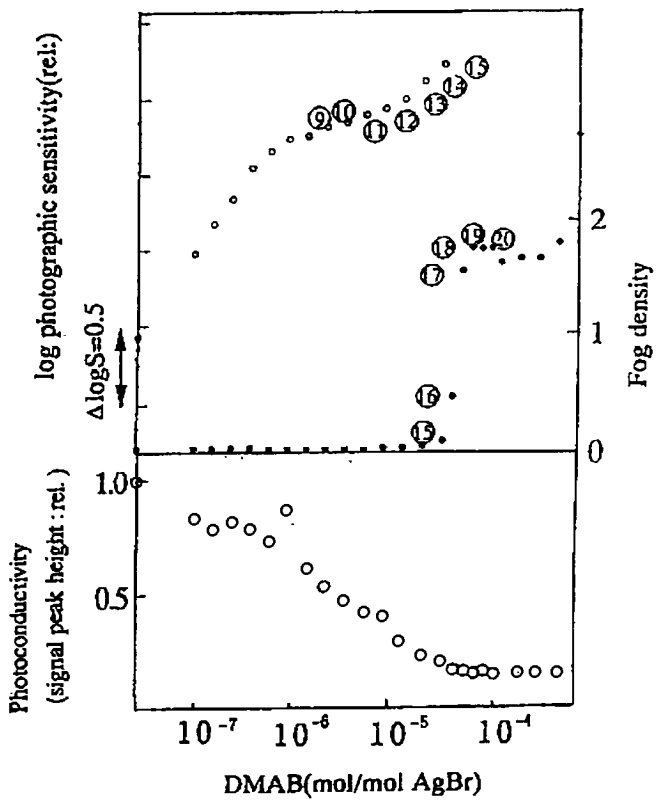

Fig. 2.6 Photographic sensitivity, fog density, and photoconductivity (measured at -100℃) of octahedral AgBr emulsion grains with diameter 0.2 μm as a function of the amount of DMAB used. (from [Tani, 1994])

Fig. 2.7 shows the diffuse reflectance spectra of thick liquid layers of the same reduction sensitized emulsions with reference to those of unsensitized emulsion. Reduction

sensitization could produce two main absorption bands peaked at 474 nm and around 540 nm. As shown in Fig. 2.6, silver clusters on sample number 9 to number 15 are interpreted as electron traps and all samples after sample 17 are D_{max} fogged, so the absorption band that peaked at 474 nm corresponded to the P centers and 540 nm corresponded to fog centers.

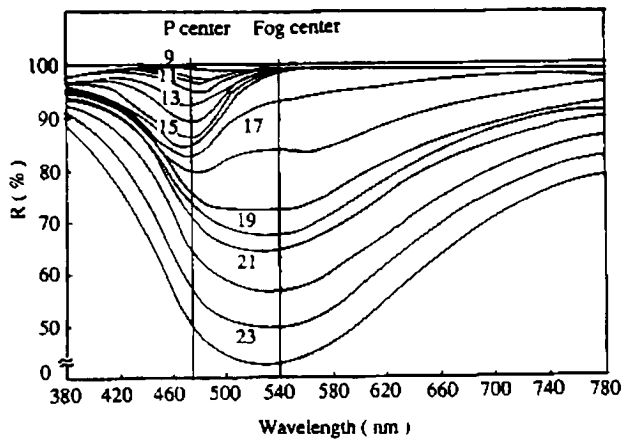

Fig. 2.7 Diffuse reflectance spectra of DMAB sensitized emulsions. The sample number corresponds to those in Fig. 2.6. (from [Tani, 1994])

The absorption spectra (Fig. 2.8) of silver clusters on the emulsion grains were derived by transforming diffuse reflectance spectra with the Kubelka-Munk (KM) equation [Herz, 1968] as shown below.

$$A = F(R) = KM = (1-R)^2/2R = c\varepsilon/S \qquad (2.1)$$

where A is the absorption, R is the diffuse reflectance of the thick layers, c is the concentration of silver clusters, and ε is the absorption coefficient of silver clusters and S is the scattering coefficient of the emulsion used. Both ε and S are functions of wavelength. The value of KM $= (1 - R)^2/2R$ in Fig. 2.8 is proportional to the product of the concentration and absorption

coefficient of those centers according to Eq. 2.1, assuming scattering coefficient is a constant. The value of KM for P centers at 474 nm and for fog centers at 540 nm are plotted as a function the amount of DMAB in Fig. 2.9, which indicates that with an increasing amount of the sensitizer, the product of the concentration and absorption coefficient of P centers increased in proportion to approximately the square of the amount of sensitizer. The lower slope in the upper region of Fig. 2.9, together with the appearance of the absorption band of fog centers, was interpreted to indicate that the sites for P centers were saturated and fog centers began to form.

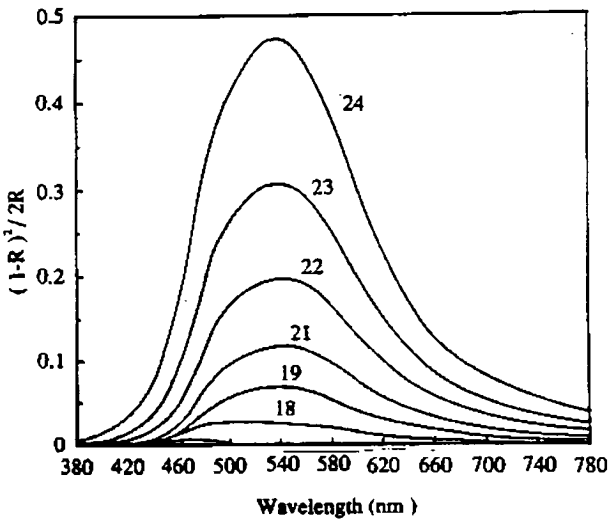

Fig. 2.8 Absorption spectra of P centers and fog centers formed on octahedral AgBr emulsion grains with diameter 0.2 μm. The numbers in this figure correspond to those in Fig. 2.6 and 2.7. (from [Tani, 1994])

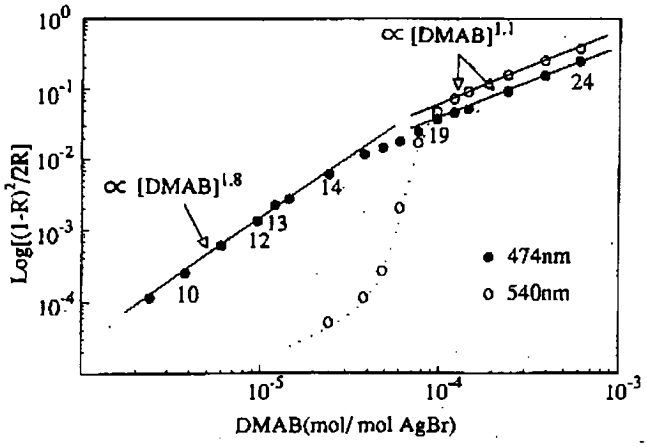

Fig. 2.9 KM value for P centers at 474 nm (•) and fog centers at 540 nm (°) as a function of the amount of DMAB used for the reduction sensitization of octahedral AgBr emulsion grains with diameter 0.2 μm. (from [Tani, 1994])

Spencer et. al. selectively reviewed many of the characteristics of chemically produced silver clusters [Spencer, 1983]. He explained that centers formed by reduction sensitization and those formed by exposure usually behave differently because of the different mechanisms whereby centers form. Exposure releases photoelectrons into the conduction band of the silver halide grains, and some of these electrons, through a complicated trapping, detrapping and ionic neutralization process, eventually form latent-image centers, which are composed of silver. Reduction sensitization, in contrast, produces silver centers without electrons entering the conduction band. Reduction sensitization centers can be either hole traps or electron traps. The sensitizer centers which are hole traps were oxidized if the silver halide grains were exposed. Trapping of holes, either directly or indirectly, by the sensitizer centers is probably the first step in the photo-oxidation. If this trapping is followed by the loss of a silver ion, the center is diminished in size, and after repetition of this hole trapping and silver-ion-ejection sequence, the center becomes too small to trigger development even after gold bathing. Some

sensitizer centers, however, can trap electrons and act as nuclei for latent image centers. He concluded that reduction sensitization induces hole traps in small octahedral grains (0.27 μm) and in larger cubic ones (0.7 μm), but induces electron traps in tabular grains (1.3 μm) and in larger octahedral ones (0.65 μm).

Chapter 3

Experimental

3.1 Emulsion preparation and sensitization.

As described previously by Hailstone, the emulsion was precipitated using the double jet method [Hailstone, 1988] and was prepared by Mr. Gary DiFrancesco. A precipitation vessel containing deionized gelatin was adjusted to pH 7.0 at 40°C. The temperature was then raised to 75°C and the pAg adjusted to 7.8 with a KBr solution. The KBr and $AgNO_3$ solutions were then pumped in at a constant flow rate for 1.5 min with the pAg held constant. The pH was then adjusted to 3.0 with HNO_3 (diluted 1 to 10) and the pAg to 8.5. The $AgNO_3$ was pumped to the vessel using an accelerated flow rate having a linear profile. Excess salt solution was stopped when the silver solution ran out, which occurred at approximately 60 min. The vessel was then cooled to 40°C, deionized phthalated gelatin added, and four washes carried out. Additional deionized gel was added and final adjustments to pH 5.6 and pAg 8.0 were made. The resulting monodisperse emulsion is composed of AgBr octahedra having a mean edge length of 0.45 μm.

Before sensitization, the emulsion was diluted by deionized gelatin solution at 40°C so as to achieve 2% Ag and 4% gel concentrations, pH was adjusted to 5.6 by NaOH or HNO_3, and pAg was adjusted to 8.0 by KBr or $AgNO_3$ solutions. Reduction sensitization was accomplished by reacting the emulsion with different levels of DMAB in 2-propanol solution or

$SnCl_2$ in water solution at 60°C for 30 min and pH sensitization (pH adjusted by 1 M NaOH) was at 60°C for 40 min. The temperature ramp conditions for DMAB and $SnCl_2$ sensitization are shown in Table 3.1. Temperature ramp for pH sensitization was similar to those in Table 3.1 except for hold and ramp time. The sensitized emulsions were stored in a refrigerator for later use.

Table 3.1. Temperature ramp conditions for sensitization.

Segment number	Aim Temp. (°C)	Control Mode	Time, (sec)
1	40	Hold	10
2	60	Ramp	800
3	60	Hold	1800
4	40	Ramp	800
5	40	Hold	600

3.2 Coating, processing, and densitometry.

The above sensitized emulsions were re-melted at 40°C, and surfactant (15% water solution of Polystep B-27) was added to each sample at the level of 2 ml/100 g emulsion. The emulsions were coated on clear acetate support at 1g Ag/m^2, 2g gel/m^2, without hardener. The film was dried over night, exposed for 10^{-2} s on EG&G model VII sensitometer with a 0 to 3.0 density, 21-step tablet incorporated into the exposure window, developed in EAA-1 for 40 min at 20°C, fixed for 3 min. Densities were measured by a Macbeth densitometer. Due to the limitation of the coating machine, D_{max} varied from one strip to another. Therefore, speed was measured at mean density, which is the average of D_{min} and D_{max}.

Fig. 3.1 is a set up schematic for processing. The films were processed as two drops simultaneously. During processing, a nitrogen gas burst from the bottom of each tube was used to agitate the solutions in the tubes and to minimize developer oxidation by air. Fig. 3.2 is the racking schematic for eight strips in one drop. A processing error test was conducted using the films cut from one coating loop.

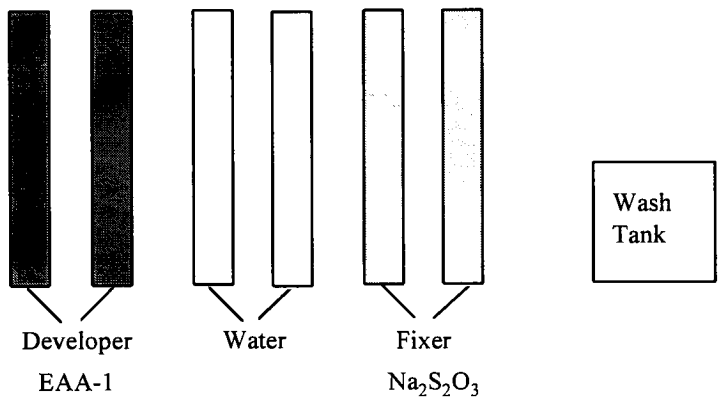

Fig. 3.1 Set up schematic for processing.

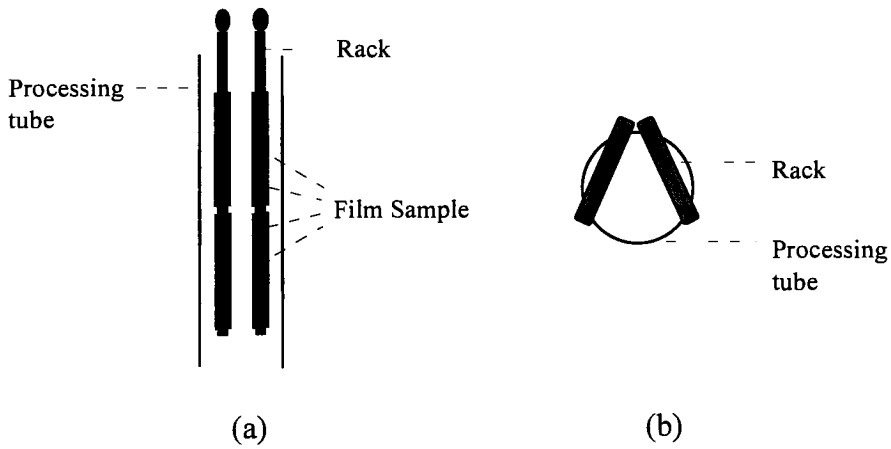

Fig. 3.2 Racking schematic for eight strips in one drop. (a) Front view. (b) Top view.

3.3 Reflectance.

The sensitized emulsions were melted and transferred into plastic cuvettes with thickness 1 cm. Reflectance spectra of unsensitized and reduction-sensitized emulsions were measured in liquid state, with reference to packed barium sulfate (also in a plastic cuvette) by a Shimadzu UV2100U spectrophotometer with an integrating sphere attachment. The samples were scanned at medium speed from 800 nm to 300 nm, with slit width 5 nm. The reflectance spectra of sensitized and/or exposed emulsion with reference to unexposed, unsensitized emulsion were obtained by subtracting the later from the former and then adding 100 (percent), wavelength by wavelength. As a result, the reflectance of a sensitized emulsion is 100% if the measured reflectance of this sample and the unsensitized emulsion are the same. The barium sulfate reference was changed once a week because its reflectance at shorter wavelength gradually deteriorates with the lapse of time.

The integrating sphere has round apertures, one for the sample and the other for the reference. As shown in Fig. 3.3, the diameter of integrating sphere aperture is bigger than the width of the cuvette, and this part is covered by the cuvette holder which is made of metal and painted black. Therefore, the so-called integrating sphere is not a complete sphere. The black spots lower the sensitivity of the instrument because they trap some of the reflected light. In addition, the cuvette holder is a little bit loose for cuvettes. Reflectance measured by this instrument is very sensitive to the position of both sample and reference cuvettes in their holders. To solve this problem, the cuvette positions were adjusted by hand so that the reflectance of all samples were the same (about 90%) at 800 nm relative to barium sulfate reference.

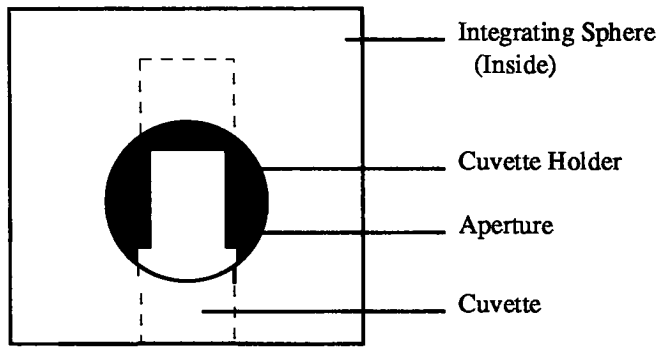

Fig. 3.3 The aperture of integrating sphere, looking from inside.

3.4 Absorption

The absorption spectra of silver clusters on the emulsion grains can be transformed from diffuse reflectance spectra with the Kubelka-Munk equation as shown below.

$$A = F(R) = KM = (1-R)^2/2R = c\varepsilon/S \qquad (3.1)$$

where R is the diffuse reflectance of the thick layers, c is the concentration of silver clusters, ε is absorption coefficient of silver clusters, and S is the scattering coefficient of the emulsion used. Both ε and S are functions of wavelength.

This transformation was done by the software called UVVIS-3000 which is available from Shimadzu. This software controls the Shimadzu UV2100U spectrophotometer which was connected to an IBM compatible 486 computer, and it also can do some calculations such as subtracting (adding, multiplying, or dividing) one spectrum from another, adding a constant to a spectrum, and smoothing a spectrum. All the reflectance spectra in this research thesis were smoothed by applying a smoothing kernel with 10 nm width before they were

transformed to absorption spectra. Each spectra was first saved as a Shimadzu data file with a suffix of ".spc". UVVIS-3000 can also transfer the ".spc" files to ASCII files in order to do further analysis using Excel or other software.

3.5 Photobleach.

The photobleach experiments were conducted by exposing emulsions in cuvettes to a tungsten-halogen light source for seconds to minutes and then running the diffuse reflectance spectra of the exposed samples. This procedure was done one sample at a time, i.e., the sample was taken to the spectrophotometer immediately after it was exposed. The data processing was the same as described in section 3.3 and 3.4.

To avoid absorption by silver the clusters directly, a 400 nm interference filter (10 nm half band width) was incorporated into the exposure window. To study chemically produced silver cluster separately, a strong electron trapping agent called methyl viologen dibromide (MV), was added to the emulsion before exposure to prevent latent-image center formation. A 1.0 neutral density filter was also used to test the reciprocity properties.

Chapter 4

Results and Discussion

4.1 Sensitometric results.

4.1.1 Processing error test.

Fig. 4.1 shows the speed distribution of the total sixteen strips used for the processing error test. The average speed is 3.005 logE, the standard deviation is 0.01

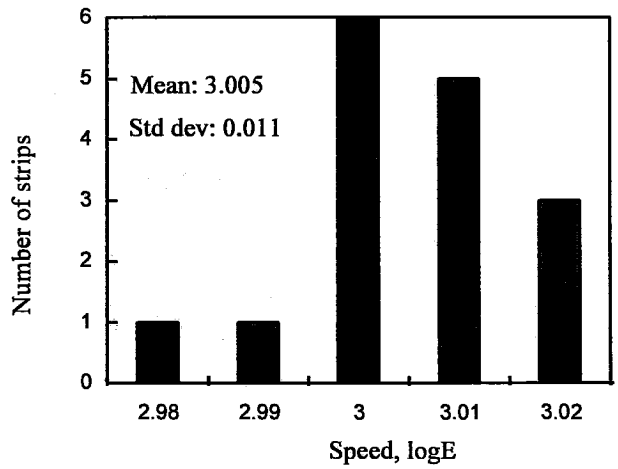

Fig. 4.1 Histogram of speed distribution in processing error test. The strips were from a coating of a 0.45 μm unsensitized octahedral AgBr emulsion, exposed on EG&G for 0.01 sec, and processed in EAA-1 for 40 min.

logE, and the measured speed error is ± 0.02 logE within 95% confidence. Fig. 4.2 is the speed distributions of the strips processed in two sets of tubes, respectively. The mean speed difference of the two sets is 0.005 logE and the speed distributions are also slightly different. These errors may be due to a different rate of nitrogen burst between the two tubes, nonuniformities in the coating, stability of sensitometer and densitometer, and the processing efficiency of both sides of the strips on a rack.

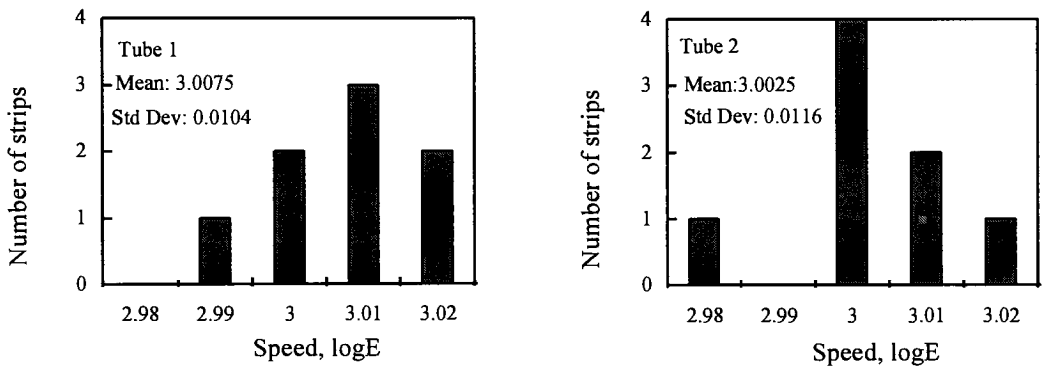

Fig. 4.2 . Speed distributions of the strips processed in two sets of tubes, respectively.

4.1.2 Sensitometric results of reduction-sensitized emulsions.

Fig. 4.3 is a plot of photographic sensitivity and fog density of reduction-sensitized octahedral AgBr emulsion grains as a function of DMAB concentration. Sensitivity for each sample is expressed by the change of speed relative to unsensitized emulsion. D-logE curves of each samples are shown in the appendix. Since all of the speed differences observed here are far beyond processing error, the speed differences can not be explained by noise.

Fig. 4.3 shows that speed continues to increase within the range of DMAB concentration used. The data indicated by solid points were obtained by processing the films on the day after sensitization and coating. The data indicated by gray points were from the first coating but processed ten days later; the empty points were obtained by coating and processing twelve days after the sensitization. Upon storage of the coated strips, speed uniformly increased but fog remained the same. However, after the sensitized emulsion was stored for twelve days and then coated, the speed increase is larger when the DMAB ccncentration is higher and the fog density started to increase as speed reached to a certain level.

Comparing Fig. 4.3 with Tani's result (Fig. 2.6), the range of DMAB concentration used corresponds to Tani's samples number 9 to 17.* Note that there is a sharp transition from no fog to D_{max} fog in Fig. 2.6, i.e. slight increase of DMAB concentration or slight increase of speed can take the emulsion from no fog to D_{max} fog. That's why fog density of Tani's sample 17 is about one third of D_{max}, but none of the solid points in Fig. 4.3 appear foggy and the last empty point appears one fourth of D_{max} fog. Roughly speaking, the results of this experiment and Tani's experiment are consistent with each other.

* The AgBr octahedral grain used in this experiment was 0.45 μm in edge length, whereas, Tani used a 0.2 μm grain in diameter. Suppose the term "diameter" Tani used to measure the size of grain is equivalent to edge length, our concentration should be 2.25 times less if we do a comparison at equal DMAB/surface area. Therefore, log(C/2.25) = logC - 0.352, i. e., 0.352 should be subtracted from logC before comparison with Tani's results. Therefore, the highest concentration in Fig. 4.3, when adjusted for differences in edge length, is about 3 times lower than Tani's sample 17.

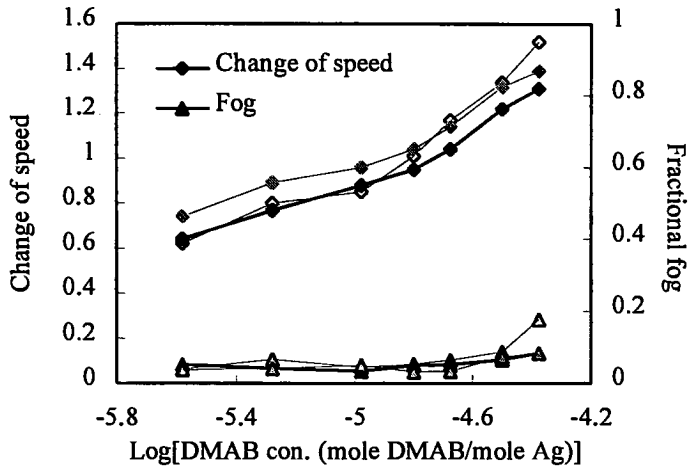

Fig. 4.3 Change of speed and fog levels as a function of log[DMAB].
The solid points: processed on the next day of sensitization and coating.
The gray points: First coating, processed ten days later.
The empty points: coated and processed 12 days after sensitization.

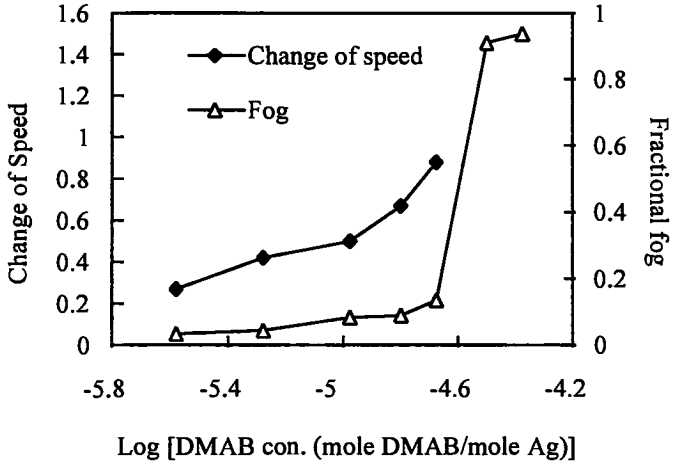

Fig. 4.4 Change of speed and fog levels as a function of log[DMAB]. This is a different DMAB sensitization with the same procedure as the DMAB sensitization in Fig. 4.3. The films were coated and processed 25 days after sensitization.

Fig. 4.4 is a plot of relative speed and fog levels as a function of log[DMAB] for another batch of DMAB sensitization with the same procedure as the DMAB sensitization in Fig. 4.3. The films were coated and processed 25 days after sensitization. Comparing the two plots, it seems that the emulsions in Fig. 4.3 are faster especially at low DMAB concentration. The difference is much more than the change due to instability. Reproducibility of $SnCl_2$ sensitization is even worse than that of DMAB sensitization. Reproducibility of a pH sensitization has not been studied. Therefore, in addition to the stability problem, more work is needed to study the reproducibility of reduction sensitization.

Fig. 4.5(a) and (b) are plots of relative speed and fog levels as a function of $SnCl_2$ concentration or pH. For $SnCl_2$ sensitization, unlike DMAB sensitization, speed increases with the concentration of $SnCl_2$ up to a maximum speed increase of 1.1 logE. When this speed has been reached, more sensitizer could not invoke more speed increase but did increase the fog density. After the coated films were stored for 11 days, the speed and fog slightly increased. However, after the emulsion samples were stored for 13 days, then coated and processed, both the speed and fog decreased. The pH sensitization series resulted in a speed gain similar to that for DMAB and $SnCl_2$.

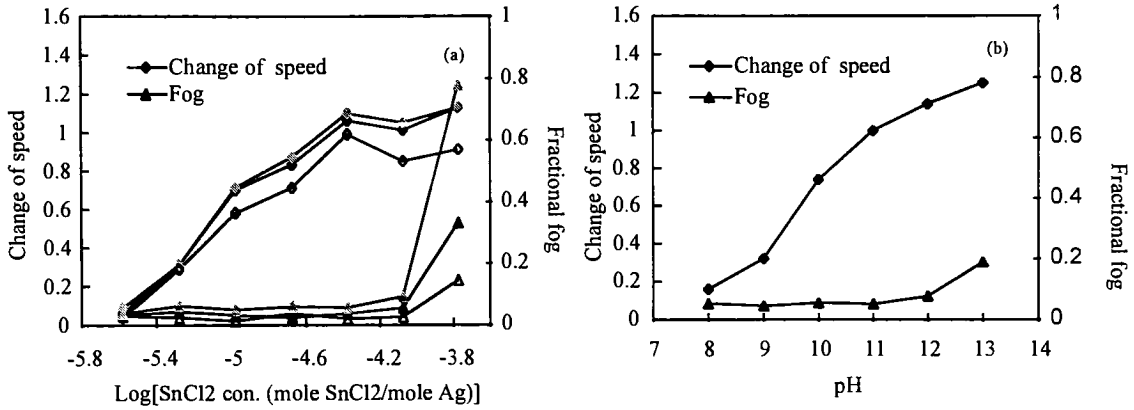

Fig. 4.5 Change of speed and fog levels as a function of log[$SnCl_2$] or pH.
The solid points: processed on the next day of sensitization and coating.
The gray points: first coating, processed 11 days later.
The empty points: coated and processed 13 days after sensitization.

4.2 Reflectance and absorption.

Fig. 4.6 is typical reflectance spectra for the same DMAB sensitization series as described in Fig. 4.3. The spectrum with smallest valley depth corresponds to the sample sensitized with the smallest amount of DMAB, and that with biggest valley depth corresponds to the sample sensitized with the largest amount of DMAB. The reflection decreases with the concentration of DMAB. The minimum reflection occurs at about 476 nm for the sample with the highest DMAB level. The minimum reflections of the samples sensitized with lower level of DMAB shift to longer wavelength. This shift is consistent with Tani's work [Tani, 1994] shown in Fig. 2.7.

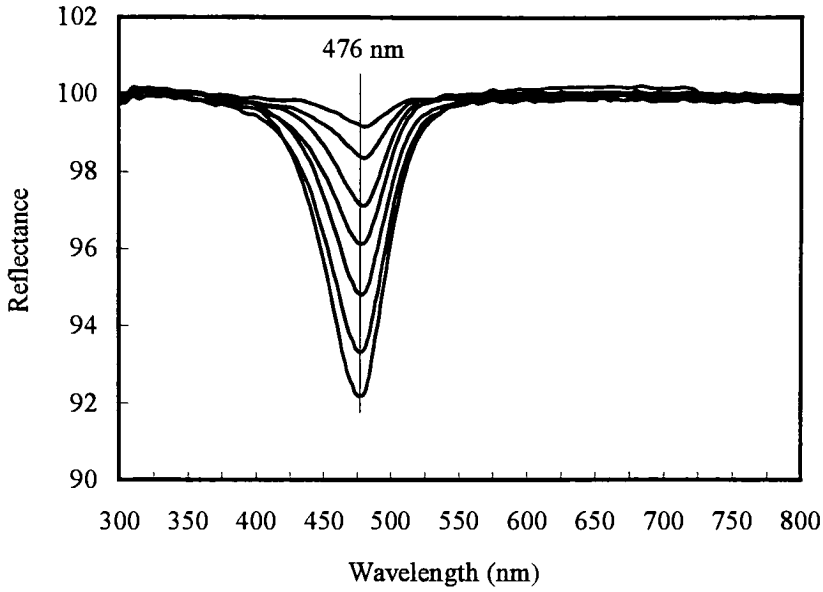

Fig. 4.6 Reflection spectra for the DMAB sensitization series described in Fig. 4.3.

Fig. 4.7 shows the relationship between relative speed and minimum reflectance of each DMAB-sensitized sample. The two sets of data, diamonds and triangles, are from the same DMAB sensitization, but the coating and processing date, and the date of running the reflectance spectra are different (see caption of Fig. 4.7 for details). This figure shows that as speed increased upon storage, the reflectance peak also increases. The trend lines for the two sets of data are very close to each other. Such a trend line can be used as a look up table. Therefore, film speed could be approximately determined by simply running a reflectance spectrum of the emulsion.

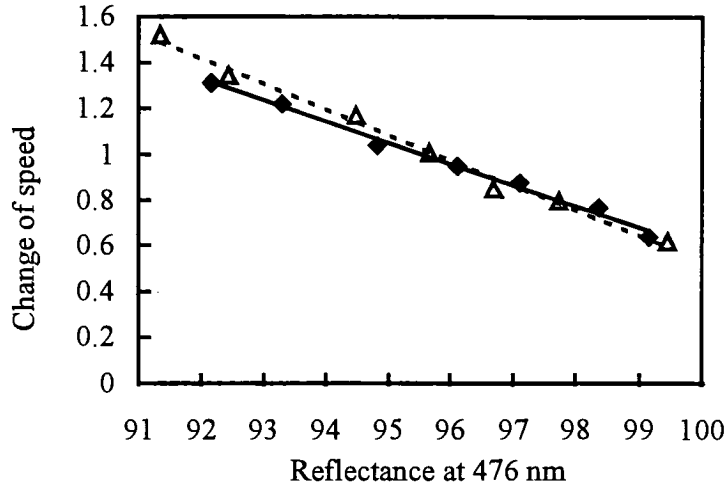

Fig. 4.7 Relationship between change of speed and reflectance at 476 nm of each DMAB sensitized samples. Diamonds: spectra run and films processed on the next day of sensitization and coating. Triangles: spectra run and films coated and processed 12 days after sensitization. The solid line is a first order least-square fit of the diamonds. The dotted line is a first order least square fit of the triangles.

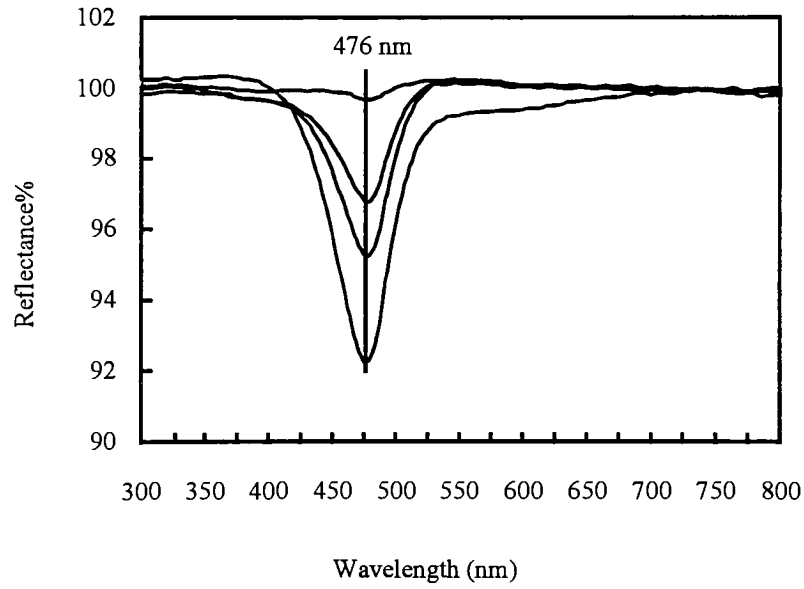

Fig. 4.8 Reflectance curves for the $SnCl_2$ sensitization series described in Fig. 4.5(a).

Fig. 4.8 is reflectance spectra of the $SnCl_2$ sensitization series described in Fig. 4.5(a). The spectra are very similar to Fig. 4.6, except that the valley depth is smaller compared with the same mole concentration of DMAB. Only four spectra are shown in Fig. 4.8 because the signal of the three lowest concentrations are too weak to be detected. The reflectance spectra of the pH-sensitized emulsions could not be obtained, since the signals were too weak. Fig. 4.9 and Fig. 4.10 shows absorption spectra obtained from Fig. 4.6 and Fig. 4.8 using the Kubelka-Munk transform, respectively.

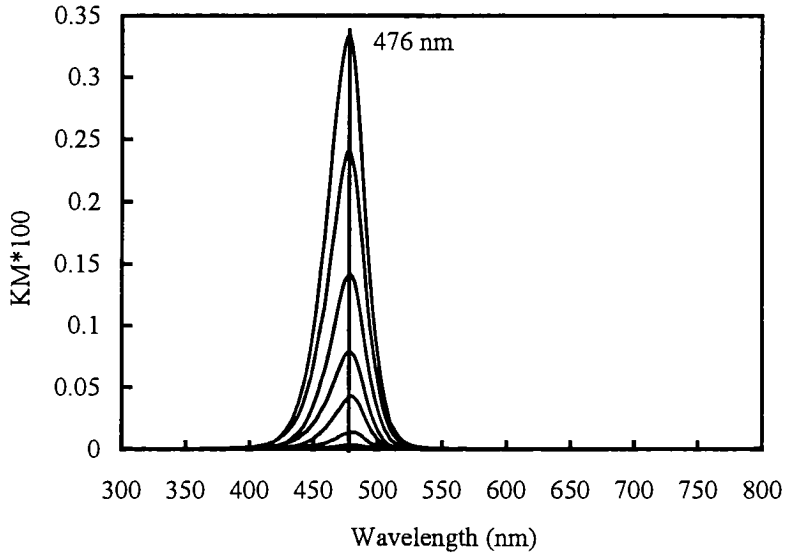

Fig. 4.9 Absorption (KM) spectra of DMAB sensitized emulsions obtained from Fig. 4.6.

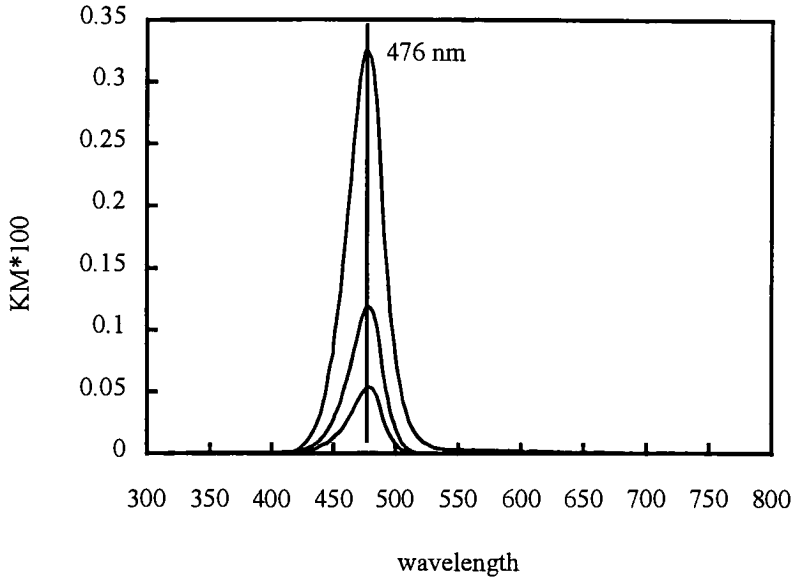

Fig. 4.10 Absorption (KM) spectra of $SnCl_2$ sensitized emulsions obtained from Fig. 4.8.

4.3 Relationship between absorption (KM) and sensitizer concentration.

According to Eq. 3.1, if KM at a certain wavelength is plotted against silver cluster concentration c, the slope or tangent of the curve gives ε/S. However, the silver cluster concentration c is unknown. Therefore, a relationship between silver cluster concentration c and sensitizer concentration [sens] must be first established.

Table 4.1 indicates the average number of DMAB molecules per grain. The calculations are as follows:

DMAB molecules/sample = (mole DMAB/mole Ag) × (mole Ag/sample) × 6.02×10^{23}

AgBr weight/sample = total weight/sample × Ag% × MW_{AgBr}/AW_{Ag} *

* MW_{AgBr}: molecular weight of AgBr.
AW_{Ag}: atom weight of Ag.

AgBr volume/sample = (AgBr weight/sample) / AgBr density

Number of grains/sample = (AgBr volume/sample) / grain volume

DMAB molecules/grain = (DMAB molecules/sample) / (Number of grains/sample)

Table 4.1 Calculation of the number of DMAB molecules per grain.

index	C (mole/mole Ag)	mg DMAB	mg/mole Ag	number of molecules	molecule/grain
1	0				
2	2.64×10^{-6}	2.875×10^{-3}	0.155	2.94×10^{16}	2694
3	5.27×10^{-6}	5.749×10^{-3}	0.311	5.87×10^{16}	5389
4	1.05×10^{-5}	1.150×10^{-2}	0.622	1.17×10^{17}	10778
5	1.58×10^{-5}	1.725×10^{-2}	0.932	1.76×10^{-17}	16167
6	2.11×10^{-5}	2.230×10^{-2}	1.243	2.35×10^{17}	21556
7	3.16×10^{-5}	3.449×10^{-2}	1.864	3.52×10^{17}	32334
8	4.22×10^{-5}	4.599×10^{-2}	2.486	4.70×10^{17}	43112

The average number of DMAB molecules per grain, in the range from a few thousand to tens of thousand, indicates that either only a very small amount of sensitizer added actually reacted to form silver clusters, or many silver clusters formed on the surface of each grain. The former conclusion cannot be proved unless the unreacted DMAB concentration could be analyzed. Spencer's investigation supports the assumption of many centers per grain [Spencer, 1981]. In addition, Spracklen gave the result that there could be as many as thousands to tens of thousands of S^{2-} atoms/μm^2 on the surface of silver halide grain, depending on the sulfur sensitizer level and exposure time [Spracklen, 1966]. The AgBr grain used in our experiments is 0.45 μm in edge length, which leads to a surface area of 0.70 μm^2. Although the size of silver sulfide aggregates $(Ag_2S)_n$ is unknown, it's likely that there are a thousands of silver sulfide aggregates per grain at optimum concentration. Analogous to

sulfur sensitization, the production of thousands of silver clusters per grain by DMAB is plausible.

In order to derive a relationship between the sensitizer concentration and the silver cluster concentration, we make the following assumptions:

1. The reaction between the reduction sensitizer is irreversible, i.e., there is no equilibrium.

2. The reaction goes to completion.

3. There are no side reactions.

4. The oxidized sensitizer cannot react with the silver clusters.

5. The number of Ag^+ is large enough to be considered constant throughout the reaction.

6. One sensitizer molecule provides α electrons and β sensitizer molecules produce one silver cluster.

7. Only one type of silver cluster is produced.

Then

$$\beta\text{sens} \rightarrow Ag_{\alpha\beta} \qquad (4.1)$$

where β can be fractional. The sensitizer concentrations and silver cluster concentrations are related as follows:

$$[\text{sens}]/\beta = [Ag_{\alpha\beta}] \qquad (4.2)$$

The right hand side is c. Therefore

$$[\text{sens}]/\beta = c \qquad (4.3)$$

$$[\text{sens}]/\beta = KM \times S/\varepsilon \qquad (4.4)$$

$$KM = [\text{sens}] \times \varepsilon/(S\beta) \qquad (4.5)$$

$$\log KM = \log[\text{sens}] + \log(\varepsilon/(S\beta)) \qquad (4.6)$$

This means that KM and [sens] are linearly related. Therefore, the plot of logKM vs log[sens] should be linear with slope 1.0.

Table 4.2 summarizes data related to KM and [sens] for a typical DMAB sensitization series, and Fig. 4.11 shows the relationships between KM and [sens] for this series. Since KM and [sens] are very small numbers (about 10^{-5} or 10^{-6}) and the software used for fitting trend lines can only show at most four decimal places, they were multiplied by 10^5 to make the calculation more convenient and more accurate.

Fig. 4.11(a) shows that the plot of KM vs [sens] is not linear over entire range, but a straight line fits well to the last five points ($R^2 = 0.9974$) and Eq. 4.7 describes the fitted line.

$$KM \times 10^5 = 93.672 \times [\text{sens}] \times 10^5 - 59.664 \qquad (4.7)$$

KM and [sens] are linearly related as predicted by Eq. 4.5. However, the straight line has a intercept of -59.664 instead of 0. This indicates that the spectrophotometer used cannot get a detectable signal until the sensitizer concentration has reached a certain level.[♥] This lowest sensitizer concentration can be calculated from Eq. 4.7: $C(KM=0) = 6.369 \times 10^{-6}$

[♥] This was confirmed by using a better designed integrating sphere. A reflection signal about 1.3 times stronger was obtained.

Our model assumes that all silver clusters contribute to the absorption signal. In order to adjust the data to this assumption, the effective sensitizer concentration should be calculated by subtracting C(KM=0) from the real concentration of sensitizer used. This will have the effect of causing the fitted line to pass through the origin. The calculated data are shown in Table 4.2. Note that C(KM=0) is greater than the DMAB concentration of the first two samples whose absorption spectra are still detectable. Therefore, there must be some other factors that affect the value of the intercept in Eq. 4.7 or the reaction model should be slightly changed.

Table 4.2 KM and [sens] (C) data for a DMAB sensitization series.

mg/mole Ag	C(mole/mole Ag)	$C\times10^5$	$\log(C\times10^5)$	$\log(C\times10^5$ 0.637)	KM	$KM\times10^5$	$\log(KM\times10^5)$
0	0	0					
0.155	2.64×10^{-6}	0.264	-0.579		0.00004	4	0.602
0.311	5.27×10^{-6}	0.527	-0.278		0.00014	14	1.146
0.622	1.05×10^{-5}	1.054	0.023	-0.379	0.00043	43	1.633
0.932	1.58×10^{-5}	1.582	0.199	-0.024	0.00079	79	1.898
1.243	2.11×10^{-5}	2.111	0.324	0.168	0.00142	142	2.152
1.864	3.16×10^{-5}	3.164	0.500	0.403	0.00241	241	2.382
2.486	4.22×10^{-5}	4.219	0.625	0.554	0.00333	333	2.522

Fig. 4.11(b) is a plot of $\log(KM\times10^5)$ vs $\log([sens]\times10^5)$, which is similar to Tani's work [Tani, 1994] shown in Fig. 2.9. This plot does not take effective concentration into consideration. Although log(KM) and log([sens]) are linearly related as predicted by Eq. 4.6, the slope is 1.5 rather than 1. Fig. 4.11(c) is a plot of $\log(KM\times10^5)$ vs log(effective concentration$\times10^5$). The fitted line has a slope of 0.9776, which is very close to the predicted

value of 1. This result confirms that the reaction model expressed by Eq. 4.1 is correct, at least for the highest concentrations of DMAB.

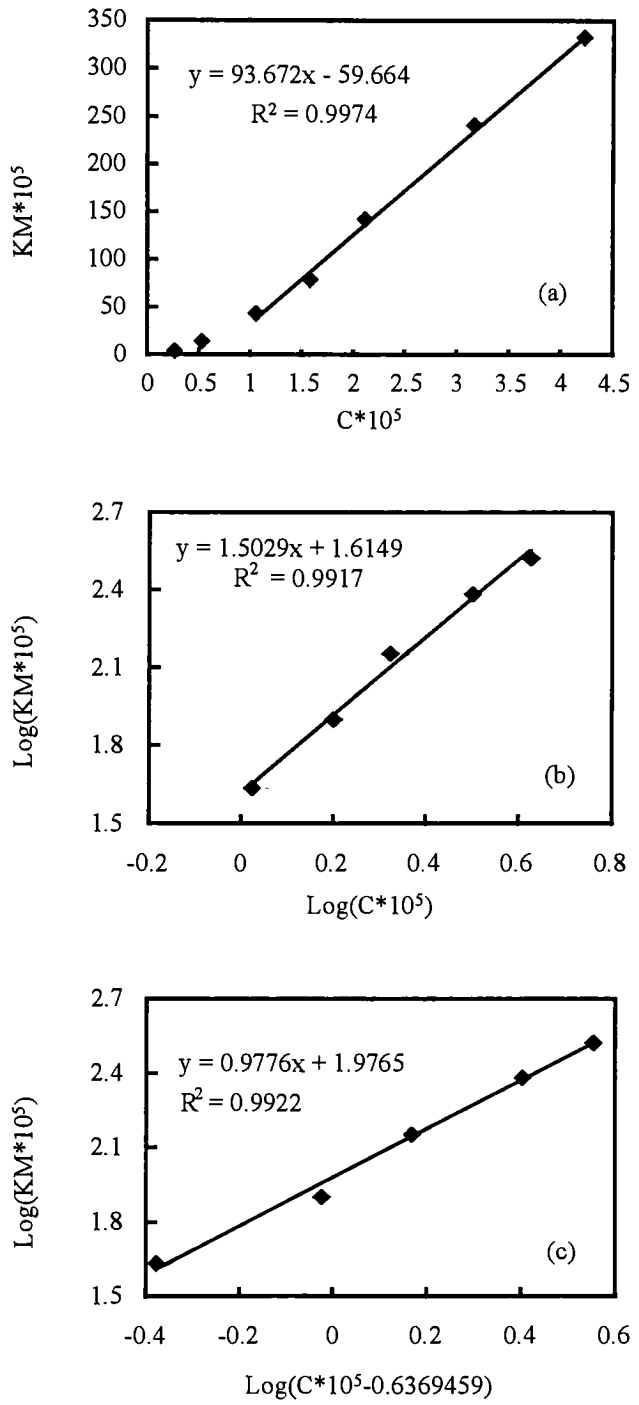

Fig. 4.11 Relationship between KM and [sens] (C) for the DMAB sensitization series.

Eq. 4.5 and Eq. 4.6 indicate that we cannot learn anything about the stoichiometry, α and β, from these plots because β is in the intercept or in the slope along with ε and S. However, we can do a similar analysis for $SnCl_2$ sensitization series and then compare the two sets of data to get some information about relative β (number of sensitization molecules to produce one silver cluster).

Table 4.3 shows KM and [sens] (C) data and Fig. 4.12 shows the relationship between KM and [sens] for the $SnCl_2$ sensitization series. The first four sensitized sample's absorption peaks are not visible in Fig. 4.10, so Fig. 4.12(b) and (c) only contains three points.

Table 4.3 KM and [sens] (C) data for the $SnCl_2$ sensitization series.

mg/mole Ag	C(mole/mole Ag)	$C\times10^5$	$\log(C\times10^5)$	$\log(C\times10^5-2.18)$	KM	$KM\times10^5$	$\log(KM\times10^5)$
0	0	0					
0.5	2.64×10^{-6}	0.264	-0.579				
1	5.27×10^{-6}	0.527	-0.278				
2	1.05×10^{-5}	1.055	0.023				
4	2.11×10^{-5}	2.111	0.324				
8	4.22×10^{-5}	4.219	0.625	0.310	0.00053	53	1.724
16	8.44×10^{-5}	8.439	0.926	0.796	0.00119	119	2.076
32	1.69×10^{-4}	16.878	1.227	1.167	0.00327	327	2.514

According to Eq. 4.6, Fig. 4.11(c), and Fig. 4.12(c), and assuming that S is a constant [Tani, 1994]:

$$\log(\varepsilon/S\beta)_{DMAB} = 1.9765 \qquad (4.8)$$

$$\log(\varepsilon/S\beta)_{SnCl2} = 1.4144 \qquad (4.9)$$

$$(\varepsilon/\beta)_{DMAB} / (\varepsilon/\beta)_{SnCl2} = 10^{1.9765}/10^{1.4144} = 3.65 \qquad (4.10)$$

If the absorption coefficient ε for the silver clusters produced by the two sensitizers is the same, then:

$$\beta_{SnCl2}/\beta_{DMAB} = 3.65 \qquad (4.11)$$

This means that it takes 3.65 times more $SnCl_2$ than DMAB to produce one silver cluster. This is consistent with the previous result that at equimolar concentration $SnCl_2$ is not as efficient as DMAB in producing a speed increase, especially at the highest concentrations (compare Fig. 4.3 and Fig. 4.5(a), Table 4.2 and 4.3). Due to the poor reproducibility of reduction sensitizations, it is hard to quantitatively compare the amount of DMAB and $SnCl_2$ used to achieve the same speed change.

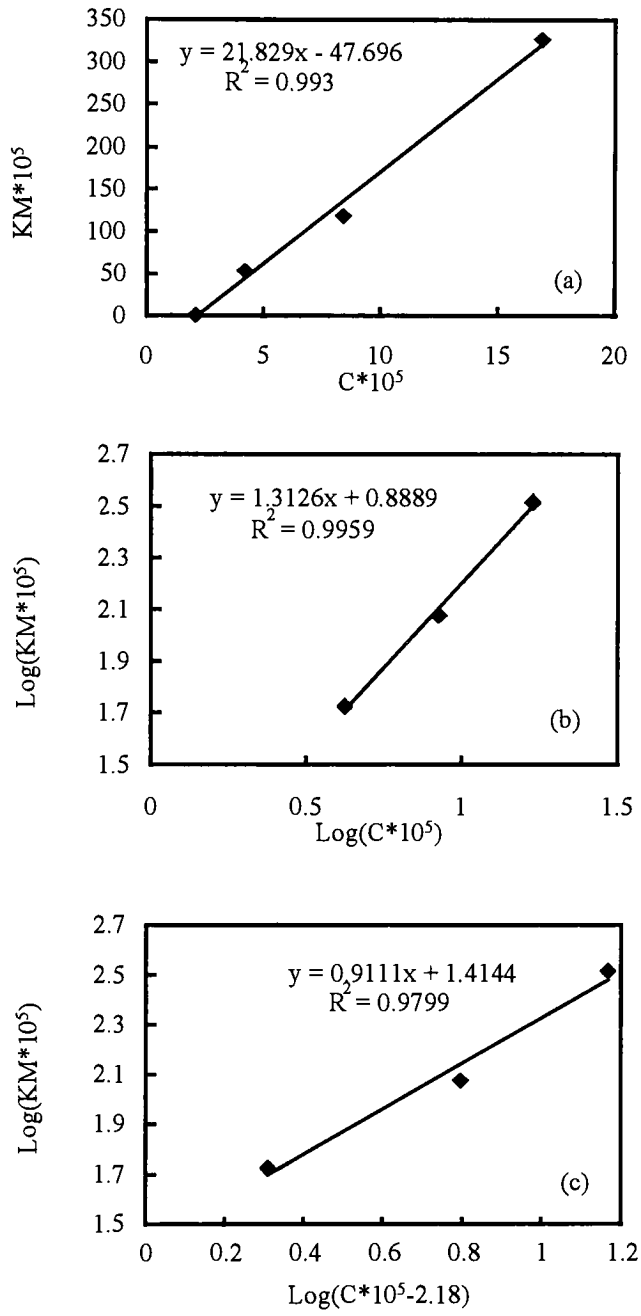

Fig. 4.12 Relationship between KM and [sens] (C) for the $SnCl_2$ sensitization series.

4.4 Photobleach of chemically produced silver clusters.

Upon exposure, silver clusters trapping electrons will grow, whereas silver clusters trapping holes will become smaller or vanish.

Electron trap:

$$Ag_n + e^- \rightarrow Ag_n$$

$$Ag_n + Ag^+ \rightarrow Ag_{n+1} \ldots \quad (4.12)$$

Hole trap:

$$Ag_n + h^+ \rightarrow Ag_n^+$$

$$Ag_n^+ \rightarrow Ag_{n-1} + Ag^+ \ldots \quad (4.13)$$

Photolytic bromine from the surrounding phase can also attack silver:

$$Ag_n + \tfrac{1}{2}Br_2 \rightarrow Ag_{n-1} + Ag^+ + Br^- \quad (4.14)$$

These two reactions, Eq 4.13 and 4.14, have of course the same origin, since bromine in the surrounding phase is created by and is in equilibrium (unless consumed) with holes in the lattice:

$$Br^- + h^+ \rightarrow \tfrac{1}{2}Br_2 \quad (4.15)$$

Therefore, given enough exposure, the reduction-sensitization produced absorption peak for an emulsion will shrink or shift to shorter wavelength if the silver clusters are hole traps, but the peak height will grow or shift to longer wavelength if they are electron traps [Ozin, 1978].*

* According to Ozin and others, the absorption bands of Ag_2, Ag_3, Ag_4, Ag_5, Ag_6, Ag_7, and Ag_∞, in an Ar matrix peaked at 412, 440, 490, 505, 520, 536, and 540 nm, respectively. However, the absorption peak is expected to be a strong function of environment.

Fig. 4.13 is the absorption spectra of a DMAB-sensitized emulsion exposed for 0 (dotted curve), 0.5, 1, 2, 4, 8, 16, 32, 64 sec, respectively. The spectrum of the unexposed sample has a single peak centered at 476 nm as we have seen in the previous section. As exposure time increases, the absorption peak shifts to longer wavelength and eventually reaches 540 nm. This is consistent with Tani's work [Tani, 1994]. Also, note that the absorption peaks of the samples exposed for 0.5 sec, 1 sec, and 2 sec are smaller than the sample with no exposure. This is an indication of photobleaching R centers. However, the broad latent image peak at 540 nm ♦ overlaps with the R center peak at 476 nm so that it is hard to resolve them and study the R center separately.

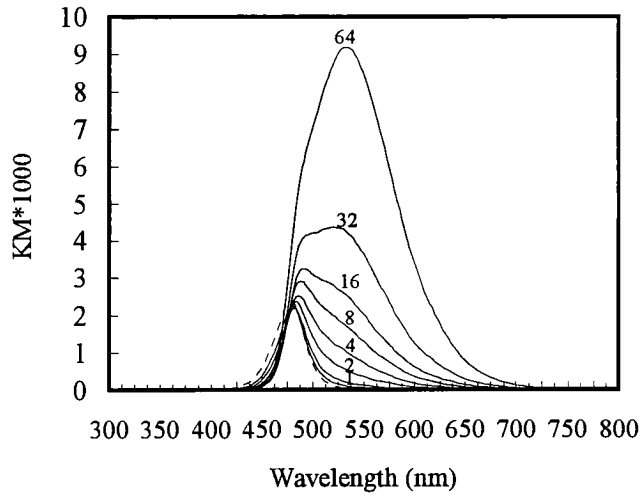

Fig. 4.13 Absorption spectra of a DMAB sensitized emulsion exposed for 0, 0.5, 1, 2, 4, 8, 16, 32, 64 sec. Dotted curve: no exposure. Solid curves: exposed.

To separate the peak at 476 nm from the overall peak, a strong electron trap or desensitizer, methyl viologen dibromide (MV) in water solution was added to the emulsion

♦ No fog centers are observed because this emulsion has been developed in EAA-1. Change of speed is 0.93 logE and the fractional fog is 0.07.

before exposure. MV is an oxidation agent. Photoelectrons were trapped by MV preventing latent image center formation during exposure. Meanwhile, MV was reduced. Fig. 4.14 shows absorption spectra of a DMAB-sensitized emulsion mixed with MV (20 g of MV per Ag mole) and exposed for 0, 1/4, 1/2, 1, 2, 4, 8, 32, 64 sec. Latent image center formation was effectively quenched by adding MV. Note that there is a weak peak at about 400 nm in each spectrum in Fig. 4.14, but no such peak was observed for emulsions without MV (see Fig. 4.9 and Fig 4.13). Fig. 4.15 shows the ultraviolet and visible absorption spectra of methyl viologen cation radical iodide (in acetonitrile and in water) and chloride (in acetonitrile) [Kosower, 1964]. The reduced form of MV has a strong and sharp absorption peak at about 400 nm and a broad peak at about 600 nm. The 600 nm peak in Fig. 4.14 is not apparent, but the 400 nm peak is likely due to the reduced MV.

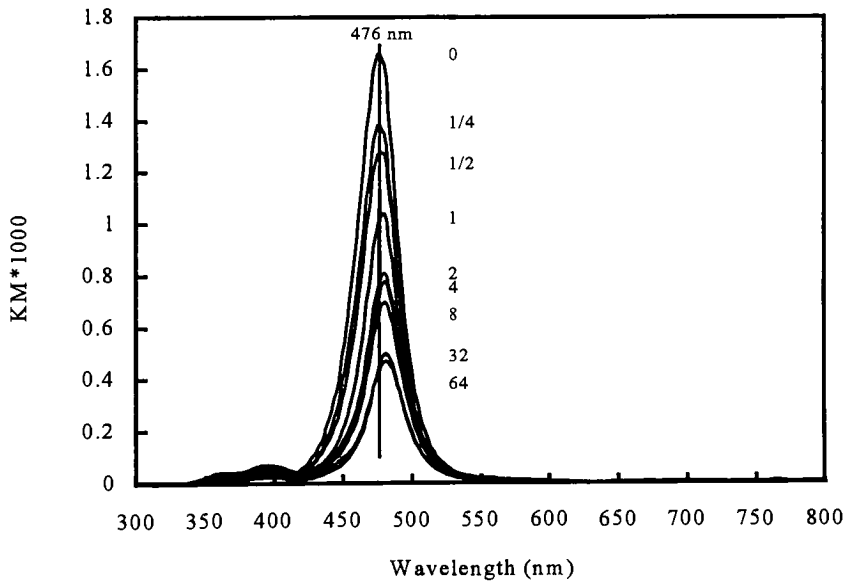

Fig. 4.14 Absorption spectra of a DMAB sensitized emulsion mixed with MV and exposed for 0, 1/4, 1/2, 1, 2, 4, 8, 32, 64 sec. The number besides each spectrum is the exposure time in seconds.

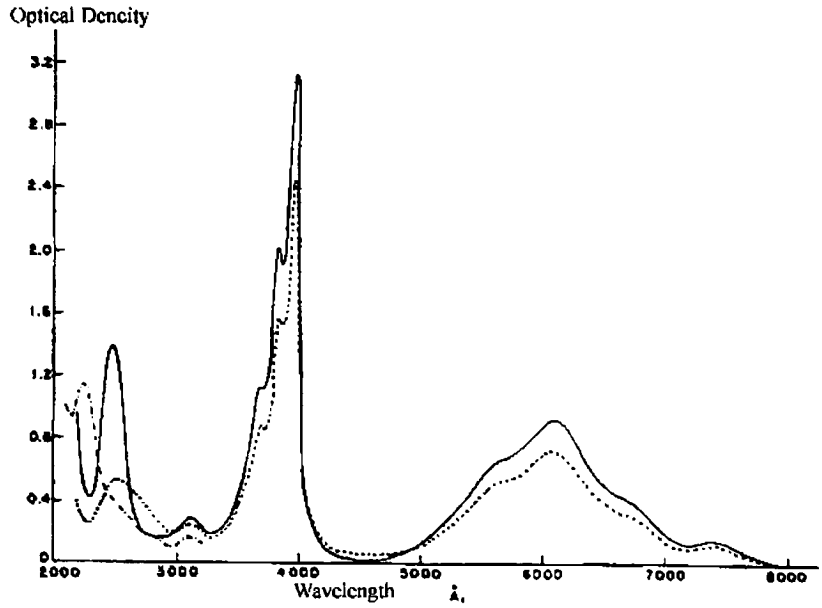

Fig. 4.15 The ultraviolet and visible absorption spectrum of methylviologen cation radical iodide (in acetonitrile. _____ and in water_._._._._.) and chloride (in acetonitrile .....). (from [Kosower, 1964])

Another feature of Fig. 4.14 is that, at short times, the absorption peak height decreases with increasing exposure time, but the spectrum of the emulsion exposed for 32 sec is almost on top of that for a 64 sec exposure, as well as for 180 sec and 360 sec exposure (not shown on Fig. 4.14). The evidence of photobleach indicates that some of the reduction sensitization centers are hole traps. However, the silver cluster absorption peak cannot be completely bleached, and the cause of the unbleachable peak is not clear. The following reasons may explain the unbleachable absorption peak:

1. The penetration depth of 400 nm light may be shorter than that of 475 nm light because silver halide absorbs more light at 400 nm. If so, the unbleachable part may be due to unexposed grains. However, this possibility is probably very low, since the

exposure (by spectrophotometer) time at about 476 nm during running the spectrum is very short compare to pre-exposure time at 400 nm.

2. Another possibility for the unbleachable peak is Ag_n in gelatin. However, it's very hard to design an experiment to separate silver bromide grain from the gelatin solution.

3. The unbleachable peak may correspond to P centers which do not have a chance to grow because MV has trapped all of the photoelectrons. Also note that the unphotobleachable centers absorb at longer wavelength than the overall peak (no exposure). Therefore, P centers and R centers are probably in different electronic environment, or perhaps P centers are larger than R centers.

To study the photobleachable silver clusters (R center) only, software called PeakFit which is available from Jandel Scientific was used to fit the spectra in Fig. 4.14 by two curves: one is the unbleachable part from the 64 sec exposure, the other is the computer generated curve that makes the overall curve fit the original spectrum well. Fig. 4.16 is an example of this curve fit. The dotted curve is the original curve before photobleach. The curve at longer wavelength is the unbleachable part, i. e., the curve with 64 sec exposure. The curve at shorter wavelength is the photobleachable part. The solid curve which is almost on top of the original is the composite curve.

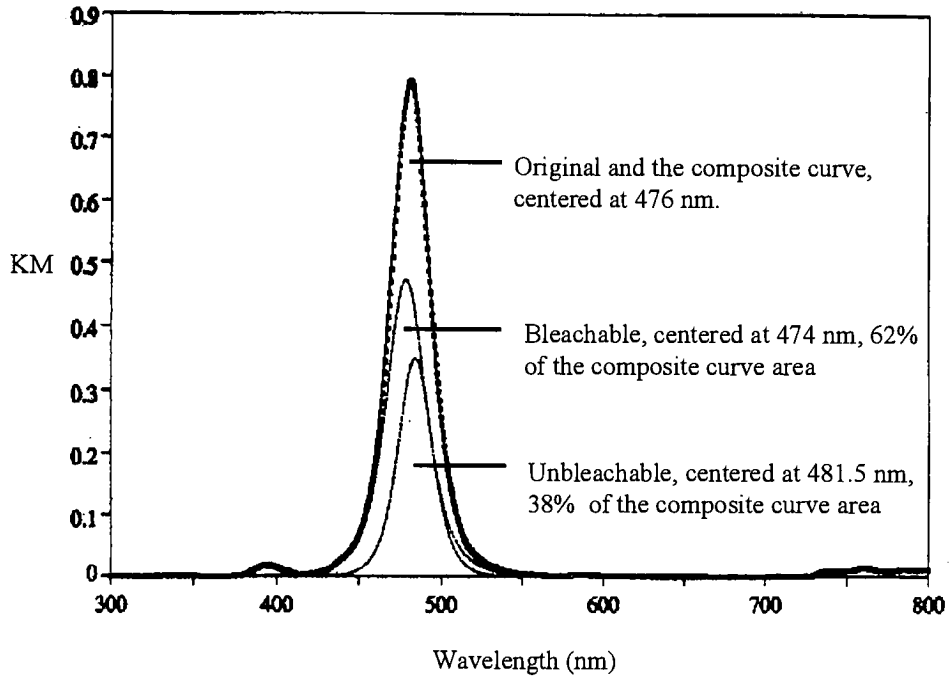

Fig. 4.16 An example of curve fit.

Each spectrum in Fig. 4.14 was fitted by two peaks as described above. Fig. 4.17 is a plot of logKM of the bleachable part against photobleach time for a DMAB sensitized emulsion mixed with MV and exposed with a 400 nm filter. The spectra obtained beyond 8 sec exposure were not analyzed because the next exposure time, 32 sec, used in this experiment has no effect on the absorption spectra (unbleachable). The bleachable peak height decreases with increasing exposure time. The data points on the plot can be fitted by two straight lines, One at shorter exposure times and with a larger negative slope, the other at longer exposure times and with a smaller negative slope. Analogous to first-order reaction kinetics, the slope of the plot is proportional to the rate of photobleach. Several possible reasons may lead to a slower rate at longer exposure times.

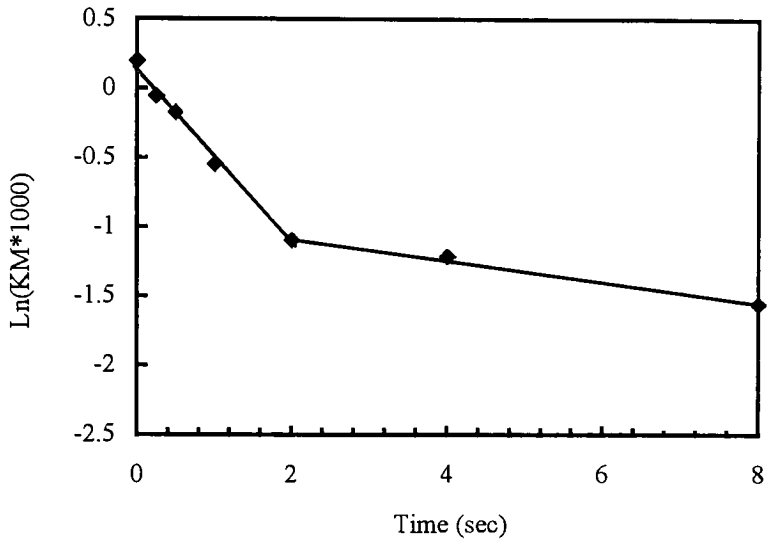

Fig. 4.17 LnKM of bleachable peak vs exposure time for a DMAB sensitized emulsion mixed with MV and exposed with a 400 nm filter (no neutral density filter).

1. The amount of MV is not enough to trap all of the electrons when exposure time is very long. In this case, photoelectrons would be trapped by P centers to form latent image centers, or recombine with photoholes. However, identical results were obtained when the MV level was increased by four times. The amount of MV appears to be sufficient to trap all the photoelectrons.

2. Reciprocity failure. If the slower rate at longer times is due to reciprocity failure, then a decrease in light intensity and an increase in exposure time should affect the results. To test the reciprocity properties, another photobleach experiment was conducted using a 1.0 neutral density filter besides the 400 nm filter, while exposure times were prolonged to about ten times. Fig. 4.18 shows the result. Fig. 4.17 and Fig. 4.18 are very similar to each other. Both of the fast and the slow components remain in Fig. 4.18. Therefore, no apparent reciprocity failure exits in photobleach process.

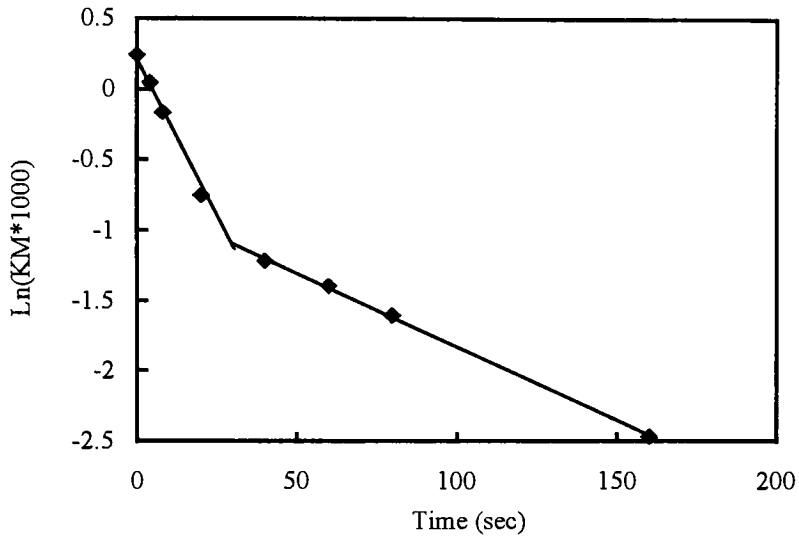

Fig. 4.18 LnKM of bleachable peak vs exposure time for a DMAB sensitized emulsion exposed with a 400 nm filter and a filter of neutral density 1.0.

3. There are probably two kinds of photobleachable centers, one with a rapid response to exposure and the other with a slow response.

The above photobleach experiments were also conducted on a $SnCl_2$ sensitized emulsion. Similar results were obtained. In this case, each sample of the $SnCl_2$-sensitized series emulsions was studied. Each sample was exposed until only the unbleachable silver clusters remained. Diffuse reflectance of each sample was obtained before and after exposure. The absorption spectra of the emulsion series that were not exposed were fitted by two peaks, photobleachable and unbleachable, as mentioned above.

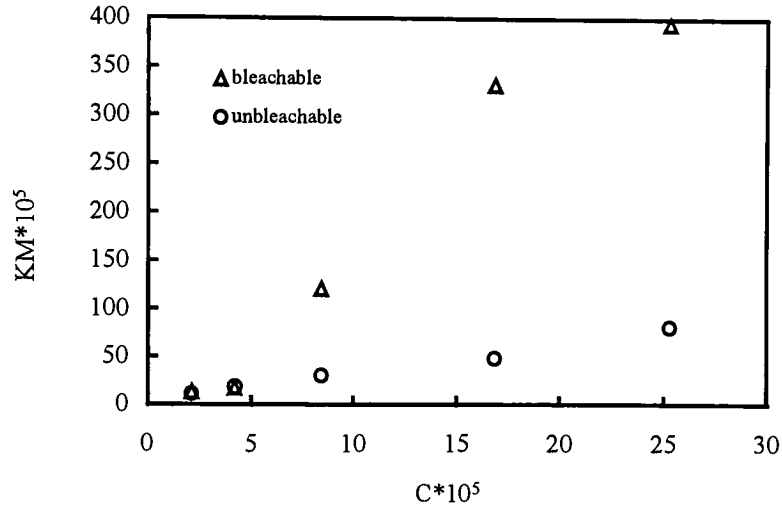

Fig. 4.19 The relationship between KM and $SnCl_2$ concentration for both photobleachable and unbleachable peaks.

Fig. 4.19 shows the relationship between KM and $SnCl_2$ concentration for both photobleachable and unbleachable part. At low $SnCl_2$ concentration, the height of the two kinds of peaks is about the same. The height of both peaks increases with the concentration of sensitizer, but the height of the bleachable peak increases much faster than that of the unbleachable peak. Assuming that the unbleachable peak is due to P centers, this result is somewhat different from previous investigations.

Both Collier and Tani made conclusion about R center and P center by measuring photoconductivity [Collier, 1979] [Tani,1994]. However, photoconductivity of the emulsion grains was measured at -100°C. The following reactions are necessary for destruction of the R centers:

$$Ag_n + h^+ \rightarrow Ag_n^+ \qquad (4.16)$$

$$Ag_n^+ \rightarrow Ag_{n-1} + Ag^+ \qquad (4.17)$$

At such low temperature, the second step may not take place. Ag_n^+ would be a good electron trap, so Ag_n can act as a recombination centers at low temperature. This can be seen in luminescence studies [De Rouck, 1983]. Therefore, photoconductivity measurements may be misleading when distinguishing R center and P center.

Palm studied surface and internal speed of a surface sensitized emulsion to determine P center and R center (see chapter 2, p. 10) [Palm, 1977]. His result could also be explained by the fact that both P centers and R centers exist simultaneously. At low sensitizer concentrations, small number of P centers may not trap all the photoelectrons. Along with R centers on the surface of silver halide grains, both the surface and internal speed may increase. The number of P centers increases with the concentration of sensitizer. Such surface electron traps compete with internal electron traps (defects, for example) so that surface speed continue to increase whereas internal speed decreases. His experiment method has it's drawback because it only sees either electron traps or hole traps, depending on which one is overwhelming.

Chapter 5

Conclusions

1. Chemically (DMAB and $SnCl_2$) produced silver clusters are not very stable upon storage. Speed and fog density increase over time.

2. Reflectance and absorption spectra of DMAB- and $SnCl_2$- sensitized emulsions were obtained and they are comparable to Tani's work [Tani, 1994]: reduction sensitizer centers at 476 nm (474 nm in Tani's paper), fog or latent image centers at 540 nm. $SnCl_2$ sensitized emulsions have smaller peaks compared with the same mole concentration of DMAB. Peaks from pH-sensitized emulsions were too small too analyze.

3. Absorption (KM) at 476 nm and the concentration (C) of DMAB or $SnCl_2$ are linearly related. Log(KM) and logC are also linearly related, with slope 1 -- as predicted by Kubelka-Munk equation and a simple reaction model. However, such data alone are not sufficient to determine the size of the silver clusters giving rise to the 476 nm peak.

4. Photobleach experiments show that some of the reduction sensitizer centers are R centers which are photobleachable, whereas some may be P centers which are non-photobleachable. In this particular experiment, both the number of R centers and the unbleachable centers increases with the concentration of sensitizer, but the number of R centers increases much faster than that of unbleachable centers.

References

Babcock T. A., Ferguson P. M., Lewis W. C., and James T. H., *Photogr. Sci. Eng,* **19**: 49(1975); *Photogr. Sci. Eng,* **19**: 211(1975).

Cash, *Photogr. Sci. Eng*, **27**: 156(1983).

Collier S. S., *Photogr. Sci. Eng,* **23**: 113(1979).

De Rouck A., *J. Photogr. Sci.* **31**: 170(1983).

Dantrich D., Granzer F., Moisar E., and Palm E., *J. Photogr. Sci.* **25**: 169(1977).

Hailstone R. K., Liebert N. B., McCleary R. T., Girolmo S. R., Jeanmaire D. L., and Boda C. R., *Journal of Imaging Science*, **32**, 113(1988).

Hamilton and Logel, *Photogr. Sci. Eng*, **18**: 507(1974).

Hamilton J. F and Beatzold R. C., *Photogr. Sci. Eng.*, **25**, 189(1981).

Hamilton J. F., in *The Physics of Latent Image Formation in Silver Halides*; Baldereschi A., Czaja W., Tosatti E., Tosi M., Eds.; World Scientific: Singapore, 1984; pp 203-224.

Herz A. H., Danner R., and Janusonis G., in *Adsorption from Aqueous Solution,* Amer. Chem. Soc., Washington, DC, 1968, p. 173.

Hirsch, *J. Photogr. Sci*, **20**: 187(1972).

James T. H., Vanselow W., and Quirk R. F., *Photogr. Sci. Eng,* **18B**: 170(1953).

Kosower E. M. and Cotter J. L., *J. Am. Chem. Soc.* **86**: 5524(1964).

Lowe W. G., Jones J. E., and Roberts H. E., in *Fundamental Mechanisms of Photographic Sensitivity*, J. W. Mitchell, Ed., (Butterworth Scientific Publications Ltd., London, 1951), p. 112.

Lowe W. G., Eastman Kodak Co. Internal Report, 1963.

Moisar E., Granzer F., Dantrich D., and Palm E., *J. Photogr. Sci.* **25**: 12(1977).

Moisar E., Granzer F., Dantrich D., and Palm E., *J. Photogr. Sci.* **28**: 7(1980).

Ozin G. A. and Huber H., *Inorg. Chem.*, **17**: 155(1978).

Palm E., Granzer F., Moiser E., and Dautrich D., *J. Photogr. Sci,* **25**: 19(1977).

Spencer H. E., Brady L.E., and Hamilton J. F., *Journal of the Optical Society of America*, **57**: 1020(1967).

Spencer H. E. and Atwell R.E, *Journal of the Optical Society of America*, **58**: 1131(1968).

Spencer H. E. and Levy M., SPSE International Symposium on Fundamentals of Latent Image Formation of Photosensitive Interfaces, Paper L-14, Lake Placid, New York, 1981.

Spencer H. E., Atwell R. E., and Levy M., *J. Photogr. Sci.* **31**: 158(1983).

Spracklen D. M., *J. Photogr. Sci.* **14**: 220(1966).

Sydow M., Karsch B., and Stolle T., *J. Inf. Rec. Mats.*, **22**: 15(1994).

Tani T., *Photogr. Sci. Eng,* **11**: 181(1971).

Tani T., *Photogr. Sci. Eng,* **16**: 35(1972).

Tani T. and Murofushi M., *Journal of Imaging Science and Technology*, **38:** 1(1994).

Appendix

DMAB Sens

8/10/95 sg

40 min. EAA1

FILE NAME: sn740

PLOT NORMALIZED: NO

SPEED METHOD: MEAN

	Shift	Fog	Speed	Speed@	Dmax
Strip 1: sn740-1	+0.00	0.07	2.69	0.60	1.13
Strip 2: sn740-2	+0.00	0.06	2.05	0.61	1.16
Strip 3: sn740-3	+0.00	0.05	1.92	0.64	1.23
Strip 4: sn740-4	+0.00	0.04	1.81	0.62	1.20
Strip 5: sn740-5	+0.00	0.06	1.74	0.63	1.21
Strip 6: sn740-6	+0.00	0.06	1.65	0.61	1.16
Strip 7: sn740-7	+0.00	0.08	1.47	0.65	1.21
Strip 8: sn740-8	+0.00	0.09	1.38	0.59	1.08

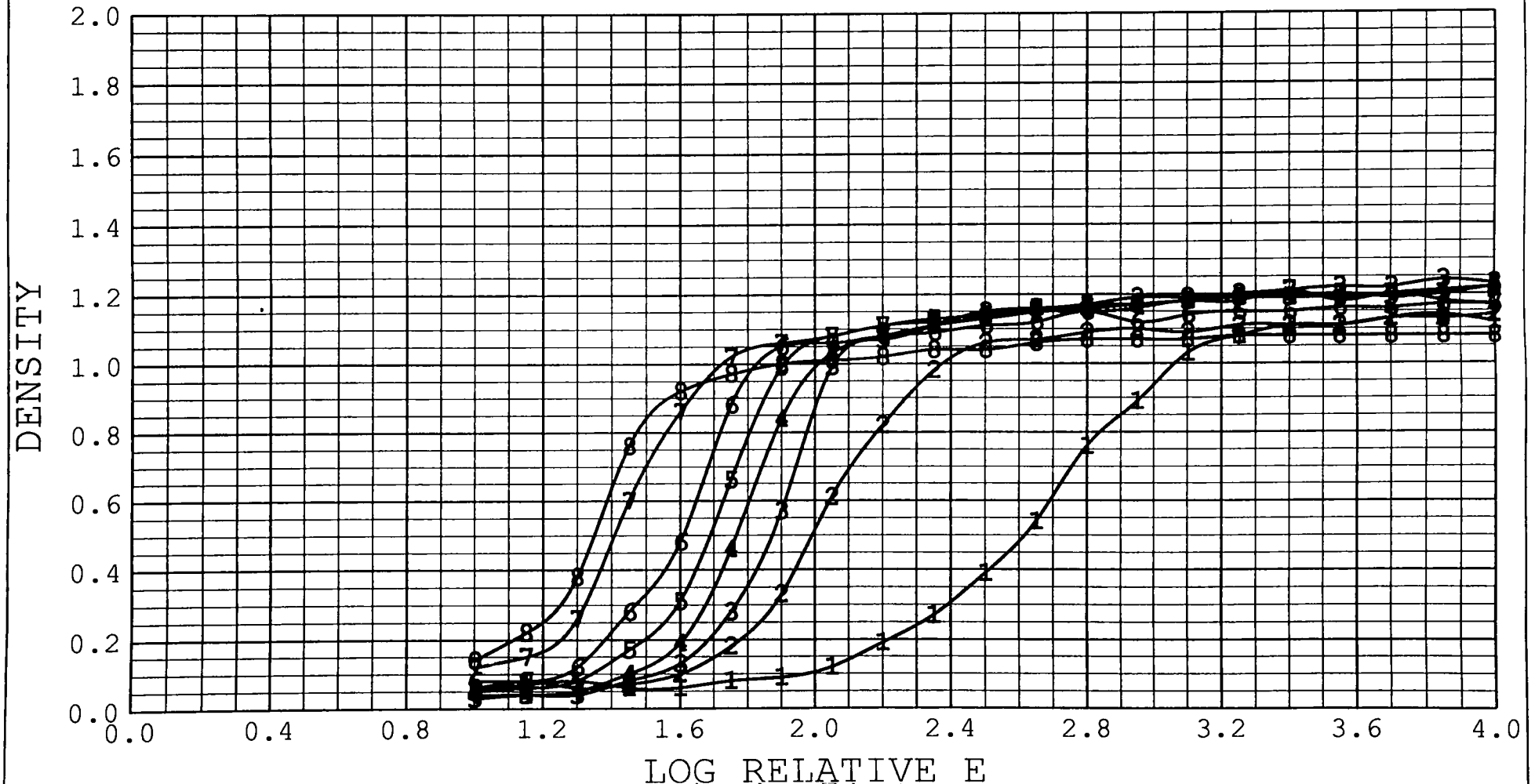

SnCl2 sens.

8/4/95 sg

40 min. EAA1

FILE NAME: sn738

PLOT NORMALIZED: NO

SPEED METHOD: MEAN

	Shift	Fog	Speed	Speed@	Dmax
Strip 1: sn738-1	+0.00	0.07	3.04	0.56	1.05
Strip 2: sn738-2	+0.00	0.06	2.98	0.64	1.23
Strip 3: sn738-3	+0.00	0.06	2.73	0.47	0.88
Strip 4: sn738-4	+0.00	0.05	2.33	0.53	1.02
Strip 5: sn738-5	+0.00	0.05	2.21	0.65	1.26
Strip 6: sn738-6	+0.00	0.07	1.98	0.63	1.18
Strip 7: sn738-7	+0.00	0.10	2.03	0.61	1.12
Strip 8: sn738-8	+0.00	0.54	1.91	0.78	1.02

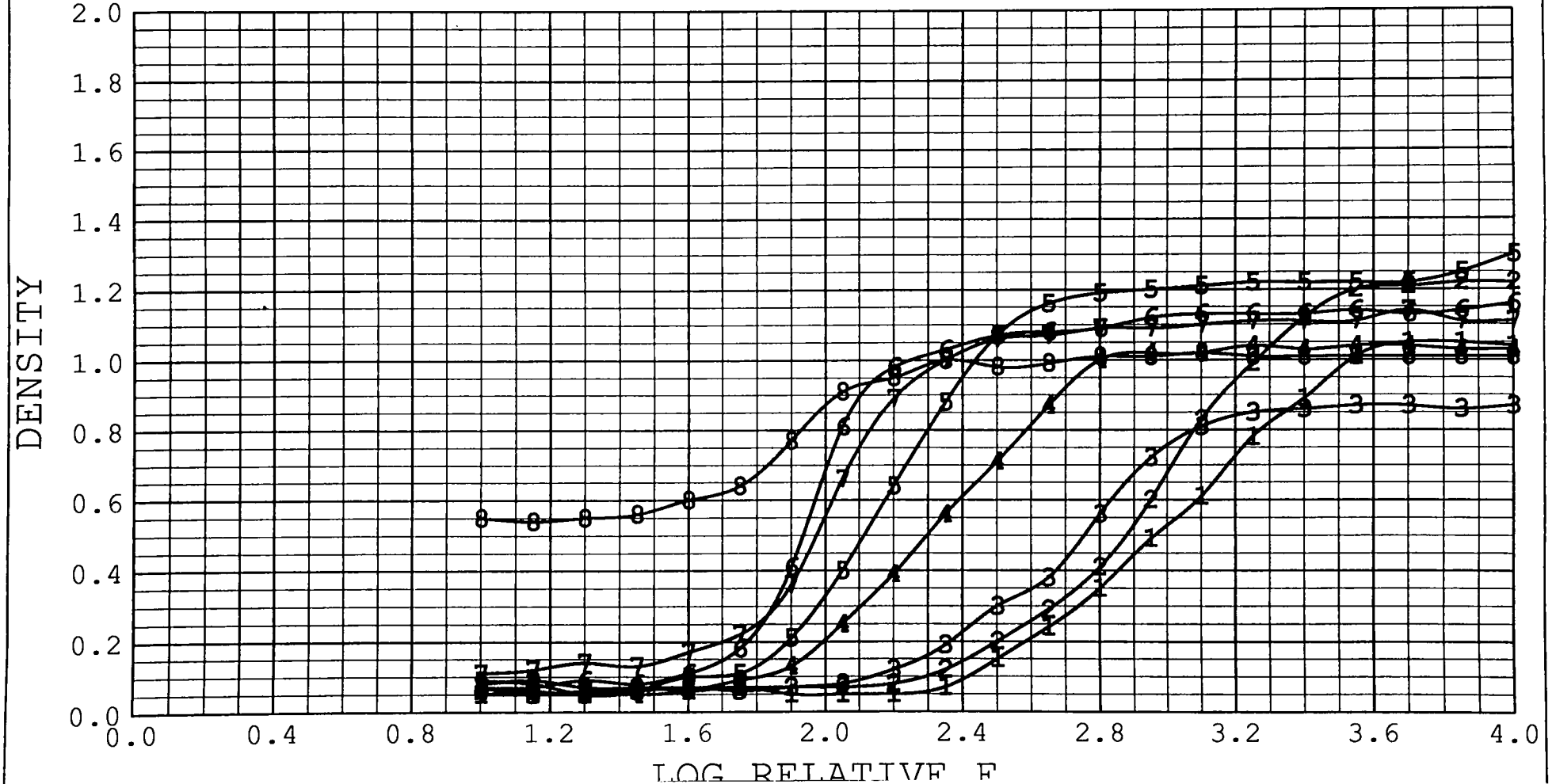

pH sens.

8/8/95 sg

40 min. EAA1

FILE NAME: sn739

PLOT NORMALIZED: NO

SPEED METHOD: MEAN

	Shift	Fog	Speed	Speed@	Dmax
Strip 1: sn739-1	+0.00	0.07	3.05	0.68	1.29
Strip 2: sn739-2	+0.00	0.06	2.89	0.59	1.12
Strip 3: sn739-3	+0.00	0.06	2.73	0.70	1.35
Strip 4: sn739-4	+0.00	0.07	2.31	0.69	1.30
Strip 5: sn739-5	+0.00	0.06	2.05	0.62	1.17
Strip 6: sn739-6	+0.00	0.05	1.91	0.35	0.65
Strip 7: sn739-7	+0.00	0.07	1.80	0.22	0.37